

**NASA CONTRACTOR  
REPORT**

NASA CR-2562

2.4/1



NASA CR-2

0061225



**STRESSES IN A WEBBED BALL, FINAL REPORT**

*L. J. Nypan*

*Prepared by*

CALIFORNIA STATE UNIVERSITY

Northridge Calif. 91324

*for Lewis Research Center*



NATIONAL AERONAUTICS AND SPACE ADMINISTRATION • WASHINGTON, D. C. • JUNE 1975





0061225

1. Report No. <b>NASA CR-2562</b>		2. Government Accession No.		3. Recipient's Catalog No.	
4. Title and Subtitle <b>STRESSES IN A WEBBED BALL</b>				5. Report Date <b>June 1975</b>	
				6. Performing Organization Code	
7. Author(s) <b>L. J. Nypan</b>				8. Performing Organization Report No. <b>None</b>	
				10. Work Unit No.	
9. Performing Organization Name and Address <b>California State University 18111 Nordhoff Street Northridge, California 91324</b>				11. Contract or Grant No. <b>NGL 05-062-002</b>	
				13. Type of Report and Period Covered <b>Contractor Report</b>	
12. Sponsoring Agency Name and Address <b>National Aeronautics and Space Administration Washington, D. C. 20546</b>				14. Sponsoring Agency Code	
15. Supplementary Notes <b>Final Report. Project Manager, Harold H. Coe, Fluid System Components Division, NASA Lewis Research Center, Cleveland, Ohio</b>					
16. Abstract  An experimental stress analysis was undertaken to evaluate stresses within cylindrically hollow reinforced webbed bearing balls proportioned for a 50 percent mass reduction. Strain gage rosettes were used to determine principal strains and stresses in the steel ball models, which were statically loaded in various orientations. Results are reported for 127 mm (5 in.) outside diameter balls under 44,500 N (10,000 lb) loads. Similitude considerations permit these results to be applied to calculations of stresses in actual size drilled bearing balls proportioned to these mass reductions.					
17. Key Words (Suggested by Author(s)) <b>Bearings; Ball bearings; Drilled ball; Webbed ball; Stress</b>				18. Distribution Statement <b>Unclassified - unlimited STAR category 37 (rev.)</b>	
19. Security Classif. (of this report) <b>Unclassified</b>		20. Security Classif. (of this page) <b>Unclassified</b>		21. No. of Pages <b>52</b>	
				22. Price* <b>\$4.25</b>	

\* For sale by the National Technical Information Service, Springfield, Virginia 22151



## TABLE OF CONTENTS

	Page
I      Summary	1
II     Introduction	2
III    Models	3
IV    Results and Discussion	5
V     Conclusion	7
VI    References	8

## LIST OF FIGURES

Figure	Page
1. Model Dimensions	9
2. Strain Gage Locations	11
3. Angles Defining Location of Strain Gages Relative to Load	13
4. Photograph of Model Positioned for Loading	14
5. Photograph of Models Used	15
6. Principal Stresses on Single Web Model Bore	16
7. Principal Stresses on Single Web Model Web	22
8. Principal Stresses on Double Web Model Bore	28
9. Principal Stresses on Double Web Model Web	34

## LIST OF TABLES

Table	Page
1. Strain Gage Locations	40
2. Strain Data, Principal Strains, Principal Stresses and Principal Angle for Webbed Ball Model.	41

## I. SUMMARY

An experimental stress analysis was undertaken to evaluate stresses within cylindrically hollow reinforced webbed bearing balls proportioned for a 50% mass reduction. Strain gage rosettes were used to determine principal strains and stresses in the steel ball models statically loaded in various orientations.

Results are reported for 127 mm (5 in) OD balls under 44,500 N (10,000 lb) loads. Similitude considerations permit these results to be applied to calculate stresses in actual size drilled bearing balls proportioned to these mass reductions.



## II. INTRODUCTION

Aircraft gas turbine engines currently operate in a speed range of 1.5 to 2 million DN (bearing bore in mm times shaft speed in rpm). It is estimated that engine designs of the next decade will require bearings to operate at DN values of 3 to 4 million. In this DN range, the reduction in bearing fatigue life due to the high centrifugal forces developed between the rolling elements and outer race becomes prohibitive.

To solve the problem of reduced fatigue life in high-speed ball bearings various methods of reducing centrifugal force have been proposed. One of these is to reduce the ball mass by "drilling" a cylindrical hole through them using electric discharge machining (EDM) techniques. Full-scale bearing tests with cylindrically hollow (drilled) balls have demonstrated that operation at speeds to 3 million DN is possible (1).<sup>1</sup> Fracture of the drilled balls has also been experienced during the operation of the full-scale bearings.

Strain gage techniques have been used successfully to evaluate stresses in the drilled ball (2). The present investigation continues the work of (2) to evaluate the effect on stresses of leaving a web or reinforcing structure within the ball instead of machining the cylindrical hole all the way through.

---

<sup>1</sup> Numbers in parentheses designate references at end of report.

### III. MODELS

Actual bearing balls dynamically loaded in a full scale ball bearing would be difficult to instrument for experimental stress analysis. The ball models used in this study were selected for ease of fabrication and instrumentation. They were turned from mild steel bar stock with a radius cutting tool to a 127 mm (5 in OD) spherical contour, bored to an ID calculated to provide the desired mass reduction of 50 per cent, and then chamfered as actual bearing balls. This procedure was used in the investigation reported in (2); so that results of the present investigation are directly comparable with the previous work. In this case, however, a reinforcing structure in the form of a web or webs was left in the bore of the model. The web was an integral part of the original ball model material in the single webbed ball. The double webbed ball model was fabricated by adhering disks with epoxy adhesive within the base of a previously used cylindrically hollow model.

Figure 1 gives model dimensions. The mild steel material simplified metal cutting. Its lack of hardness and low value of yield stress were not problems as care was taken to insure that strains were always within the elastic range. The 127 mm (5 in) model size seemed to be compatible with available 1 mm gage length strain gage rosettes and proved easy to position and load in a universal testing machine. TML ZFRA-1 (1 mm gage length) 45° strain gage rosettes were mounted on the models in locations shown in Figure 2.

The rosettes were mounted with one strain gage of each rosette aligned parallel to the axis of the hole or bore of the model. Other strain gages

on the rosette backing were then automatically aligned at  $45^{\circ}$  and  $90^{\circ}$  to the axis of the hole. A line of rosettes was thus established parallel to the bore axis on the interior of the model. As the models were symmetric about the ball mid plane perpendicular to the bore only one half of the model was strain gaged. The strain gaged half was repositioned to replace the ungaged half and reloaded to obtain a complete strain distribution. Table 1 gives actual gage locations.

The location of the rosettes relative to the vertically downward compression loads applied to the model is defined by two angles,  $\theta$  and  $\phi$ . Theta is the angle of rotation about the axis of the base from an initial orientation with the line of rosettes directly under the load ( $\theta = 0^{\circ}$  case). Figure 3 shows angles  $\theta$  and  $\phi$ . While the investigation reported in (2) presented data for cases of  $\theta = 0^{\circ}$ ,  $30^{\circ}$ ,  $60^{\circ}$ , and  $90^{\circ}$ , the  $30^{\circ}$  and  $60^{\circ}$  data served only to verify a smoothly varying continuum of stresses that a ball would experience in rolling. In practice the extreme values experienced at  $\theta = 0^{\circ}$  and  $\theta = 90^{\circ}$  are of principal interest and only these values are presented here. Exterior strains and stresses were demonstrated in (2) to be smaller than interior strains and stresses and are likewise not presented here.

Phi is the angle of inclination of the axis of the bore of the model with a horizontal plane imagined through the center of the model.  $\phi = 0^{\circ}$  is the symmetrically loaded case, while  $\phi = 40^{\circ}$  resulted in the load being applied close to the edge of the hole as may be seen in Figure 3. Data was taken at  $\theta = 0^{\circ}$ ,  $20^{\circ}$ , and  $40^{\circ}$  orientations with the load.

A 44,500 N (10,000 lb) load was used to obtain a response sufficient for accurate measurement.

Figure 4 shows a model positioned in the testing machine and Figure 5 shows the models used. The models were positioned by protractor to lines scribed on the models with a dividing head and height gage. Strains measured were very sensitive to load orientation.

Instrumentation similar to that described in (2) was used to obtain and record data.

#### IV. RESULTS AND DISCUSSION

Strains read from the recorder charts were used to compute principal strains, stresses and angles, for each rosette. These are given in Table 2.

In these tables epsilon A is the axial strain, read from the output of a strain gage mounted parallel to the axis of the hole (bore) in the model. Epsilon B is the strain  $45^{\circ}$  to epsilon A, and epsilon C is the hoop strain, read from the strain gage mounted at  $90^{\circ}$  to epsilon A. The data reads from the top down from the outermost rosette, closest to the point of load application inward past the ball center line and on out to the outermost rosette on the other side of the ball, away from the loaded point. Web strains are similarly listed from outermost rosette to center to outermost rosette.

Epsilon 1 and epsilon 2 are the computed principal strains. All strains are given in micro mm/mm (micro in/in) with  $\epsilon_1$  always being the algebraically larger (most positive) of the principal strains. Sigma 1 and Sigma 2 are the computed principal stresses in mega Newtons per square meter (kilo pounds per square inch) with Sigma 1 always the algebraically larger of the principal stresses. Alpha is the angle between  $\epsilon_A$  and  $\epsilon_1$ .

The stresses of Table 2 are shown graphically in Figures 6-9. Figure 6 shows the stresses along the bore for the single web design, while figure 7 shows the stresses along that web. The stresses along the bore for the double webbed design are shown in figure 8, and the stresses along one of these webs as shown in figure 9. In each case, the stresses are shown for two values of  $\sigma$  and three values of  $\phi$ .

Principal stresses were calculated from the measured strains using equations from Dally and Riley (3).

$$\epsilon_{1,2} = \frac{1}{2} (\epsilon_A + \epsilon_C) \pm \frac{1}{2} \sqrt{(\epsilon_A - \epsilon_C)^2 + (2\epsilon_B - \epsilon_A - \epsilon_C)^2} \quad (1)$$

$$\sigma_1 = \frac{E}{1 - \nu^2} (\epsilon_1 + \nu\epsilon_2) \quad (2)$$

$$\sigma_2 = \frac{E}{1 - \nu^2} (\epsilon_2 + \nu\epsilon_1) \quad (3)$$

with values for modulus of elasticity, E, of  $207 \times 10^9 \text{ N/m}^2$  ( $30 \times 10^6 \text{ lb/in}^2$ ) and a Poisson's ratio  $\nu$  of 0.3. Table 2 gives values of measured strain, principal strain and principal stress.

In the course of loading the models, strain was observed to be proportional to load. From equations (1), (2), and (3) above, the calculated principal stresses are then proportional to load. As stress = force/(length)<sup>2</sup> and all dimensions of a model of specified mass reduction are proportional to model outer diameter, the data in table 2 may be used to calculate stresses for similar balls as

$$\frac{\text{Stress}_1}{\text{Stress}_2} = \frac{\text{Force}_1}{\text{Force}_2} \times \left( \frac{\text{OD}_2}{\text{OD}_1} \right)^2 \quad (4)$$

Comparison of figures showing variation of stress with location in the reinforced balls with corresponding figures of reference (2) shows that both designs of webbed balls significantly affect stress levels and stress distribution. In regions close to the web (or webs) stresses are appreciably lowered when loads are applied close to a single web reinforced ball, or between or near one of the webs in the double webbed ball design. The figures also indicate that the balls can be very highly stressed by loads applied close to the edge of the holes. While this is not unexpected, the magnitudes of the principal stresses and their signs would seem to indicate that full scale bearings incorporating drilled balls should be designed with special attention to the prevention of edge loading.

## VI. CONCLUSION

The stress distribution in reinforced cylindrically hollow balls originally proportioned for a mass reduction of 50 per cent has been determined. reinforcing webs incorporated into the drilled ball reduce stresses near the reinforcement, but do not greatly reduce stresses due to loads applied near the edges of the hole where stresses are largest. If cylindrically hollow balls are used in ball bearings it seems advisable to limit load applications to less than  $20^{\circ}$  from the ball center line.

## REFERENCES

1. Holmes, P. W. Evaluation of Drilled Ball Bearings at DN Values to Three Million, Volumes I and II, NASA CR-2004 and CR-2005, 1972.
2. Nypan, L. J. Experimental Evaluation of Stresses in Cylindrically Hollow (Drilled) Balls, NASA CR-2439, August 1974.
3. Dally, J. W., and Riley, W. F., Experimental Stress Analysis, McGraw-Hill Book Company, New York, 1965

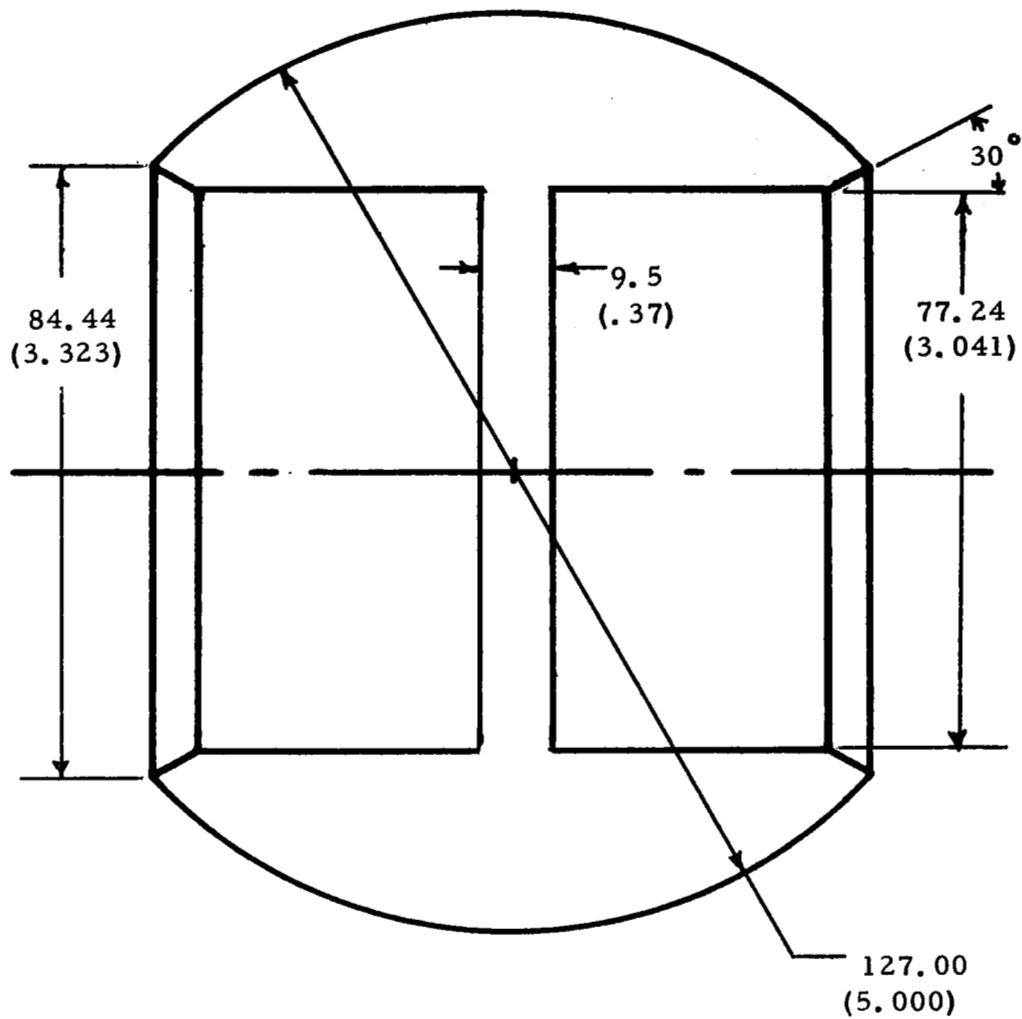


FIGURE 1 a 50% MASS REDUCTION SINGLE WEBBED BALL DIMENSIONS mm (INCHES)



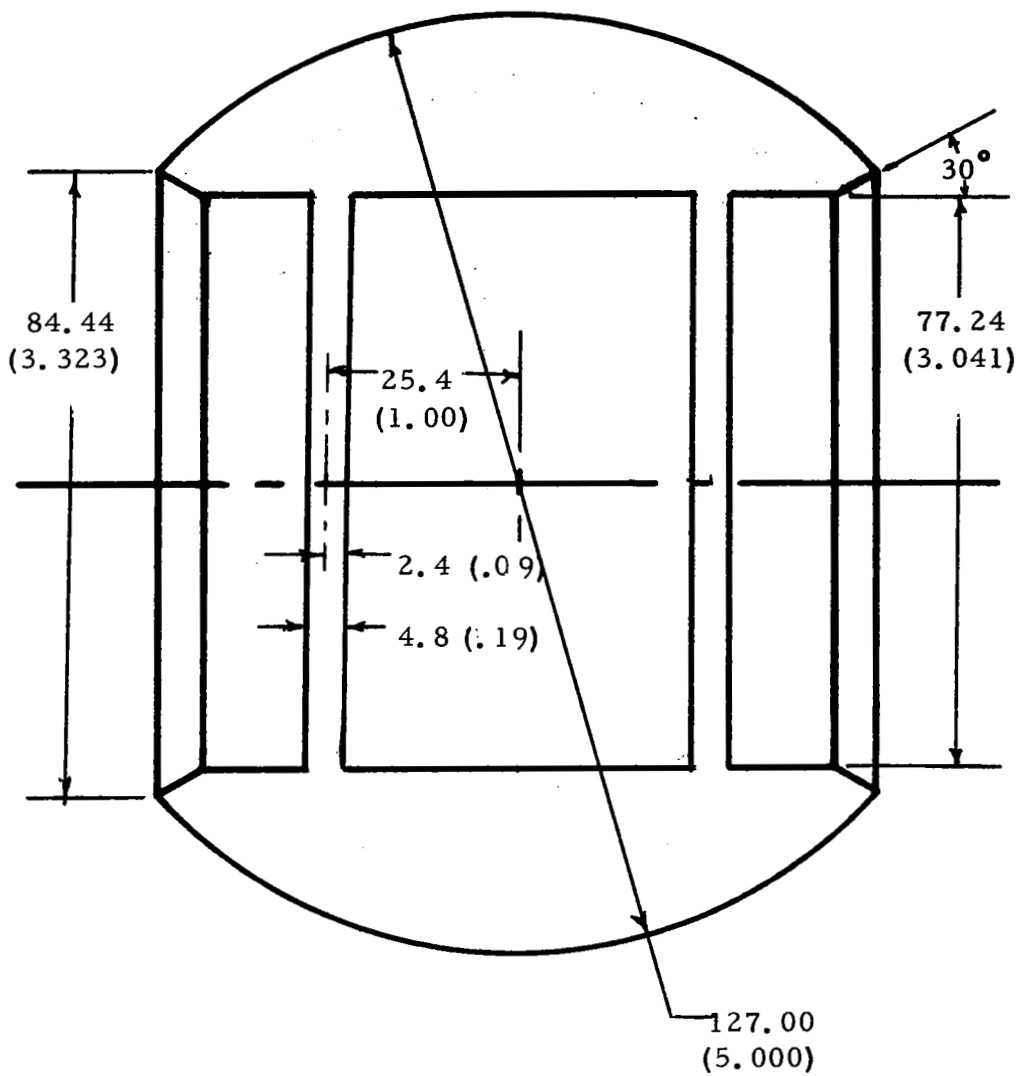


FIGURE 1 b 50% MASS REDUCTION DOUBLE WEBBED  
BALL DIMENSIONS mm (INCHES)

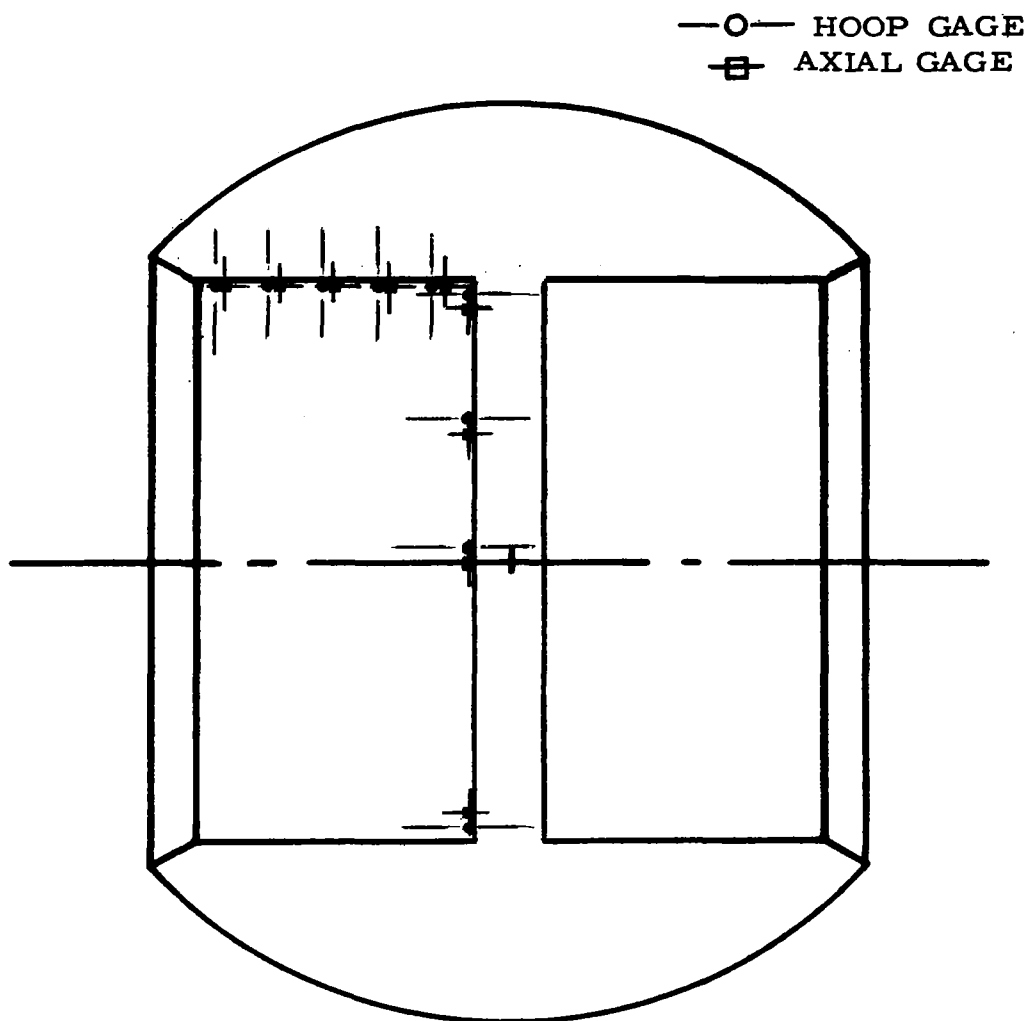
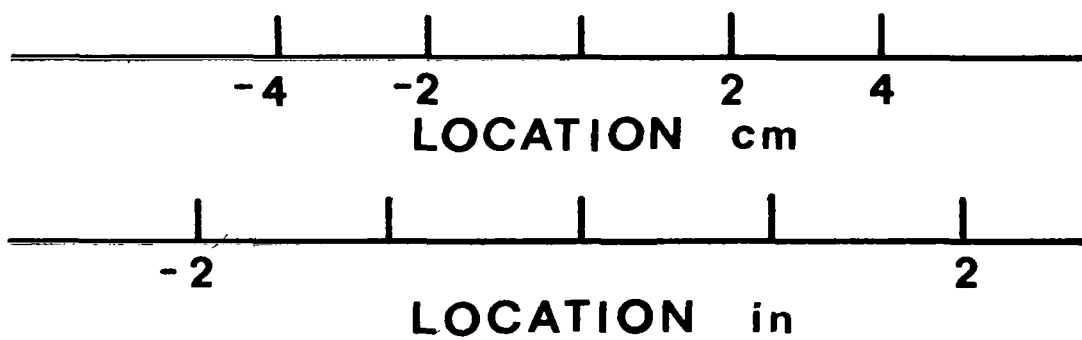


FIGURE 2 a STRAIN GAGE LOCATIONS IN SINGLE WEBBED BALL (SEE TABLE 1)



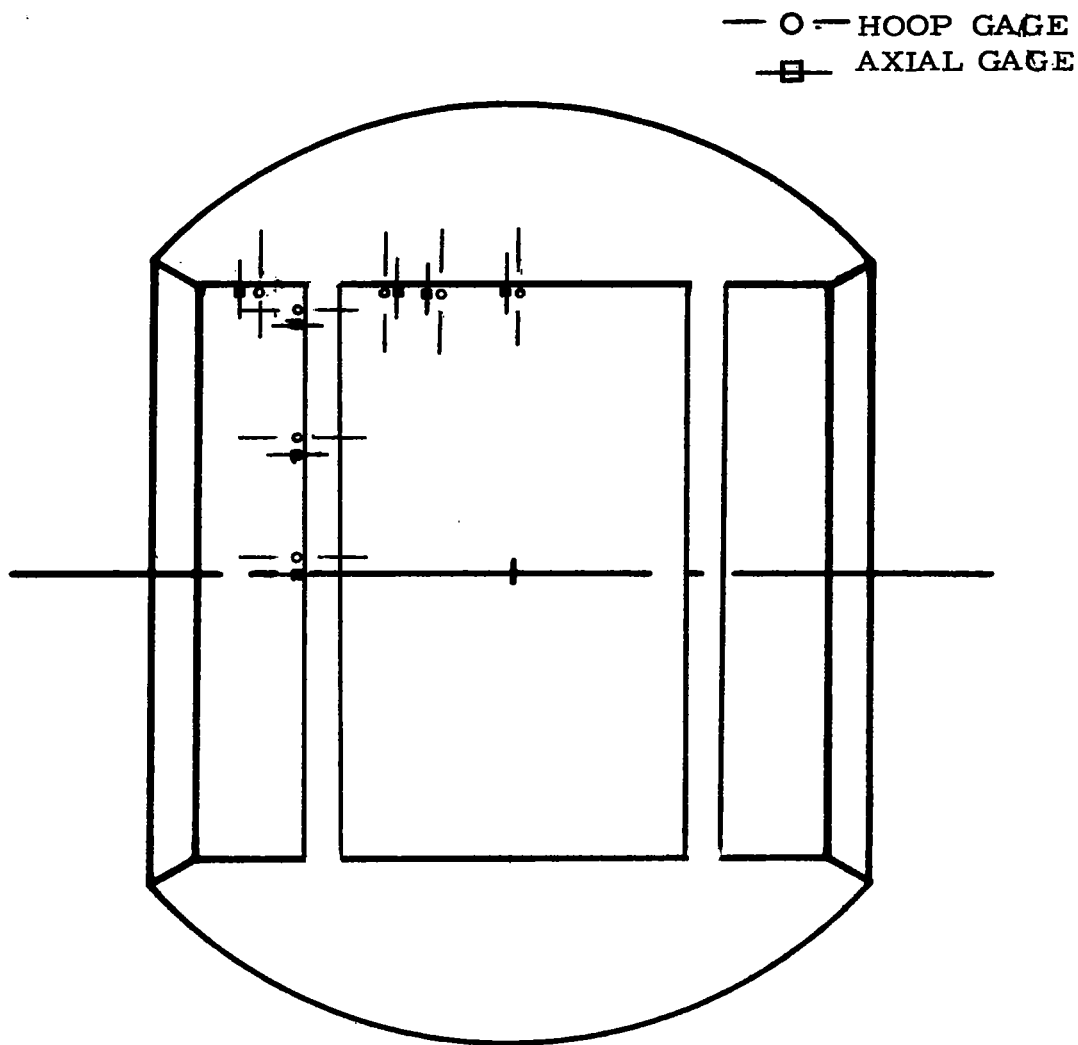
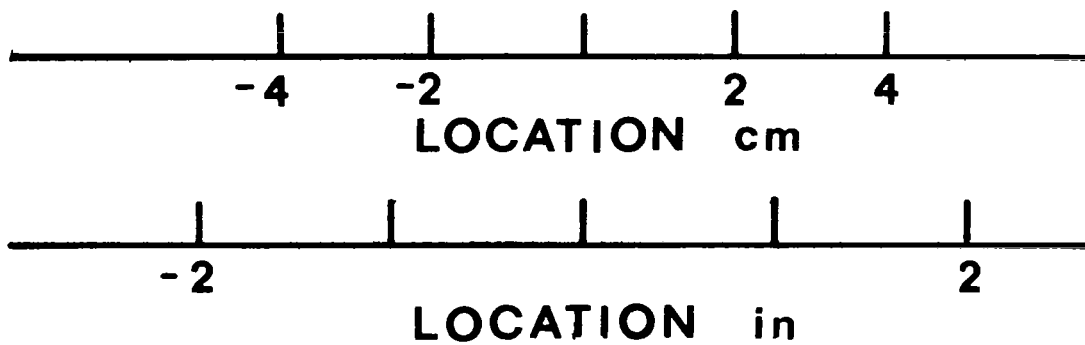


FIGURE 2 b STRAIN GAGE LOCATIONS IN DOUBLE WEBBED BALL (SEE TABLE 1)



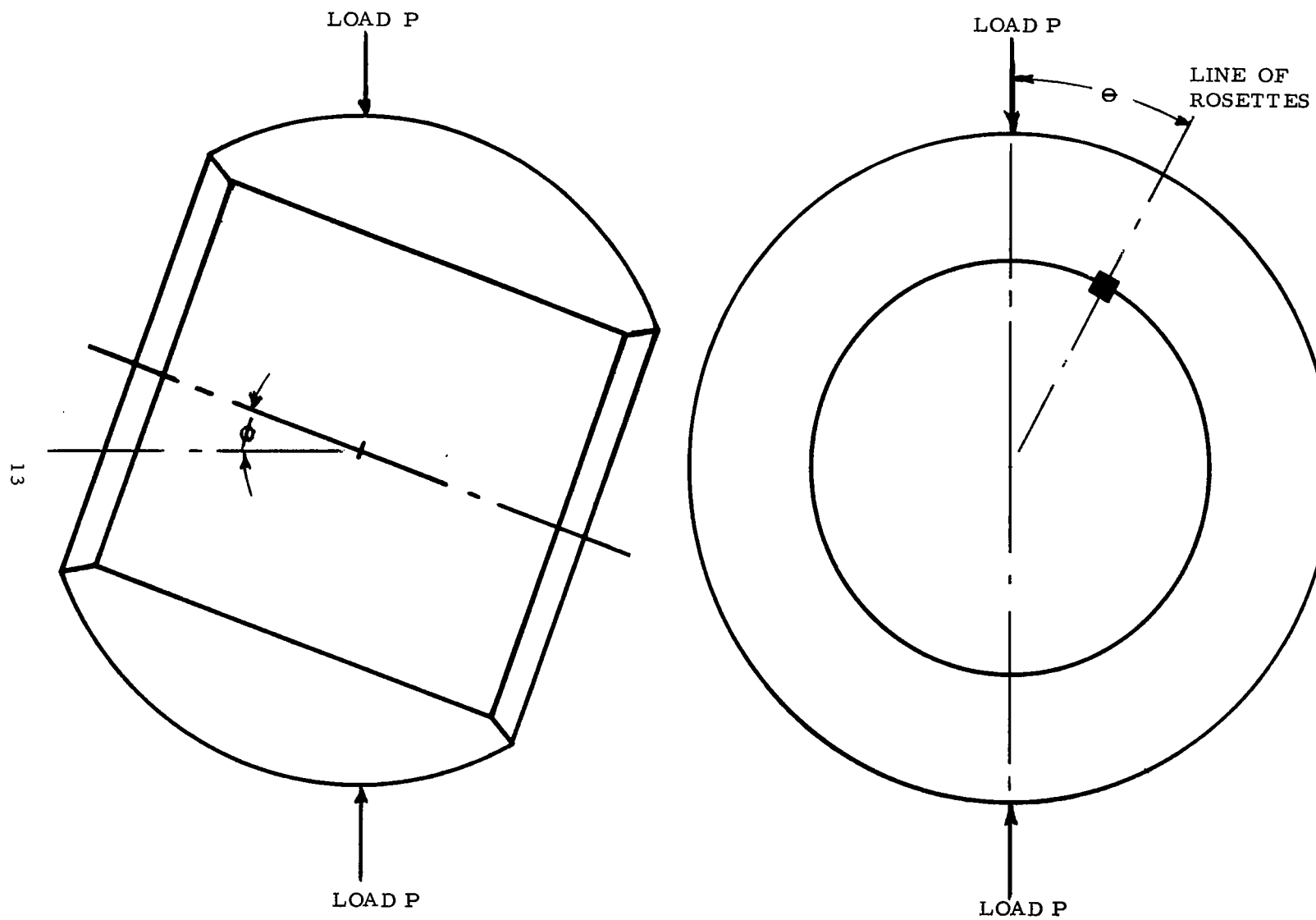


FIGURE 3 ANGLES DEFINING LOCATION OF STRAIN GAGES  
RELATIVE TO LOAD

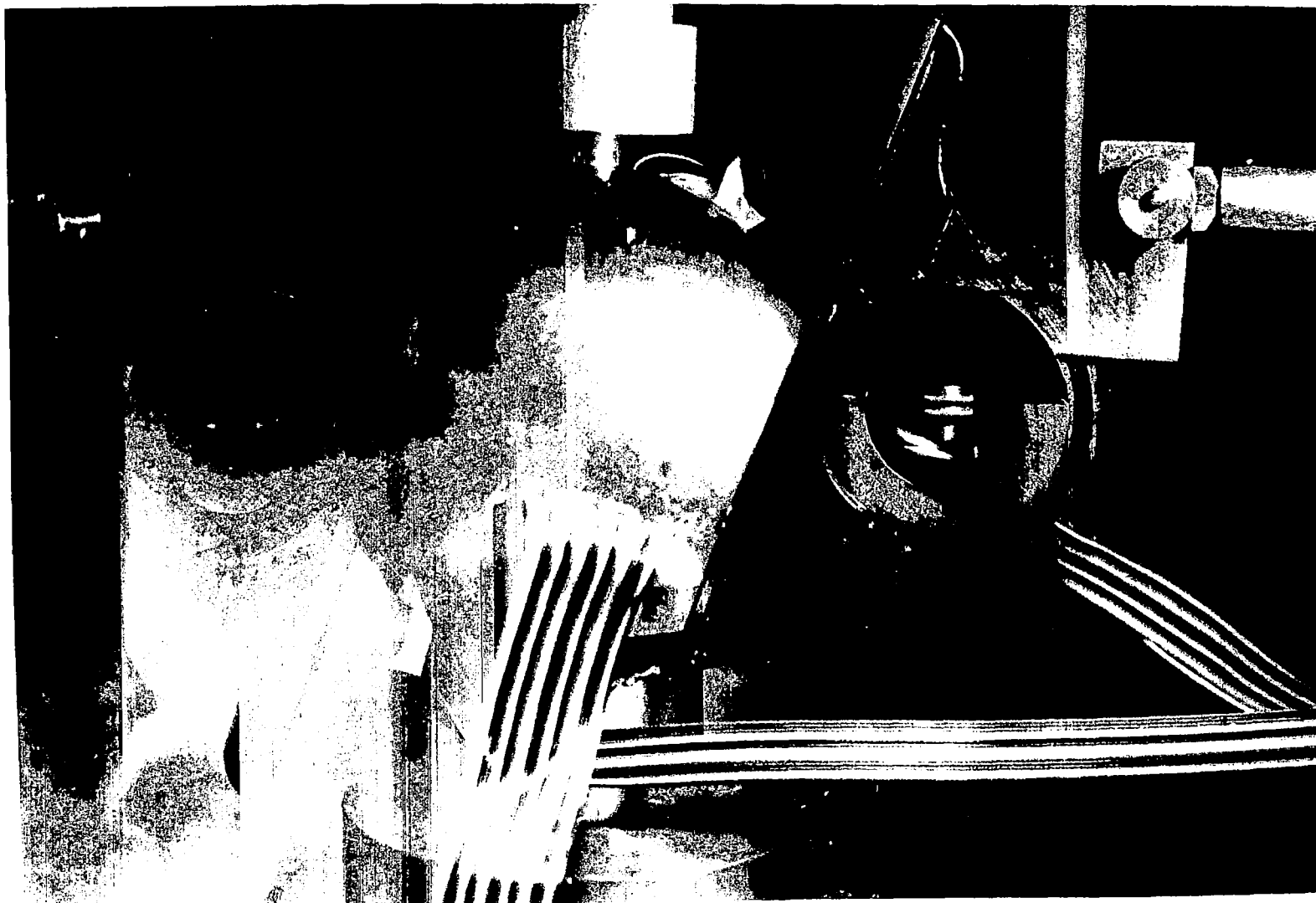


FIGURE 4 MODEL POSITIONED  
IN TESTING MACHINE

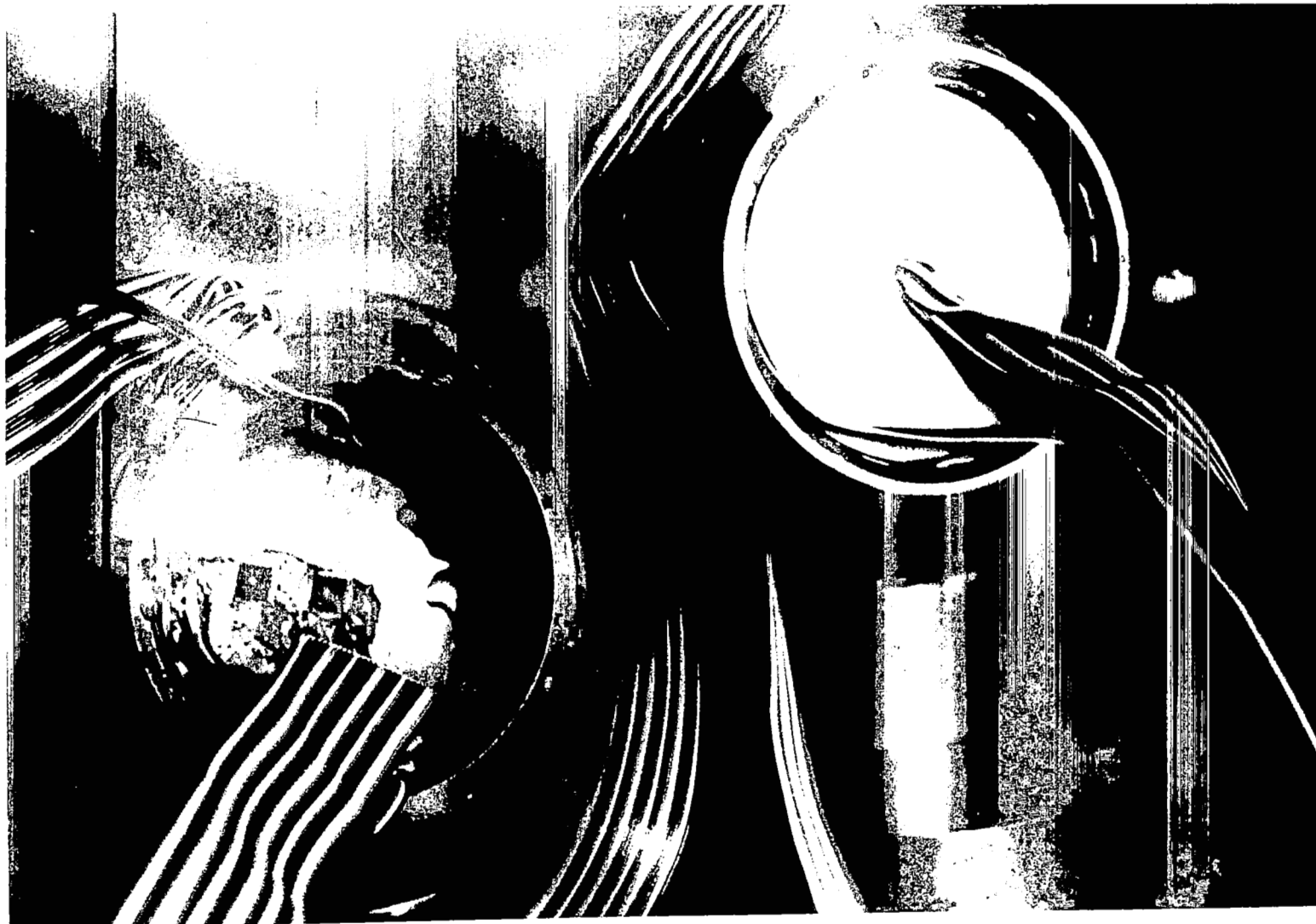


FIGURE 5 MODELS USED

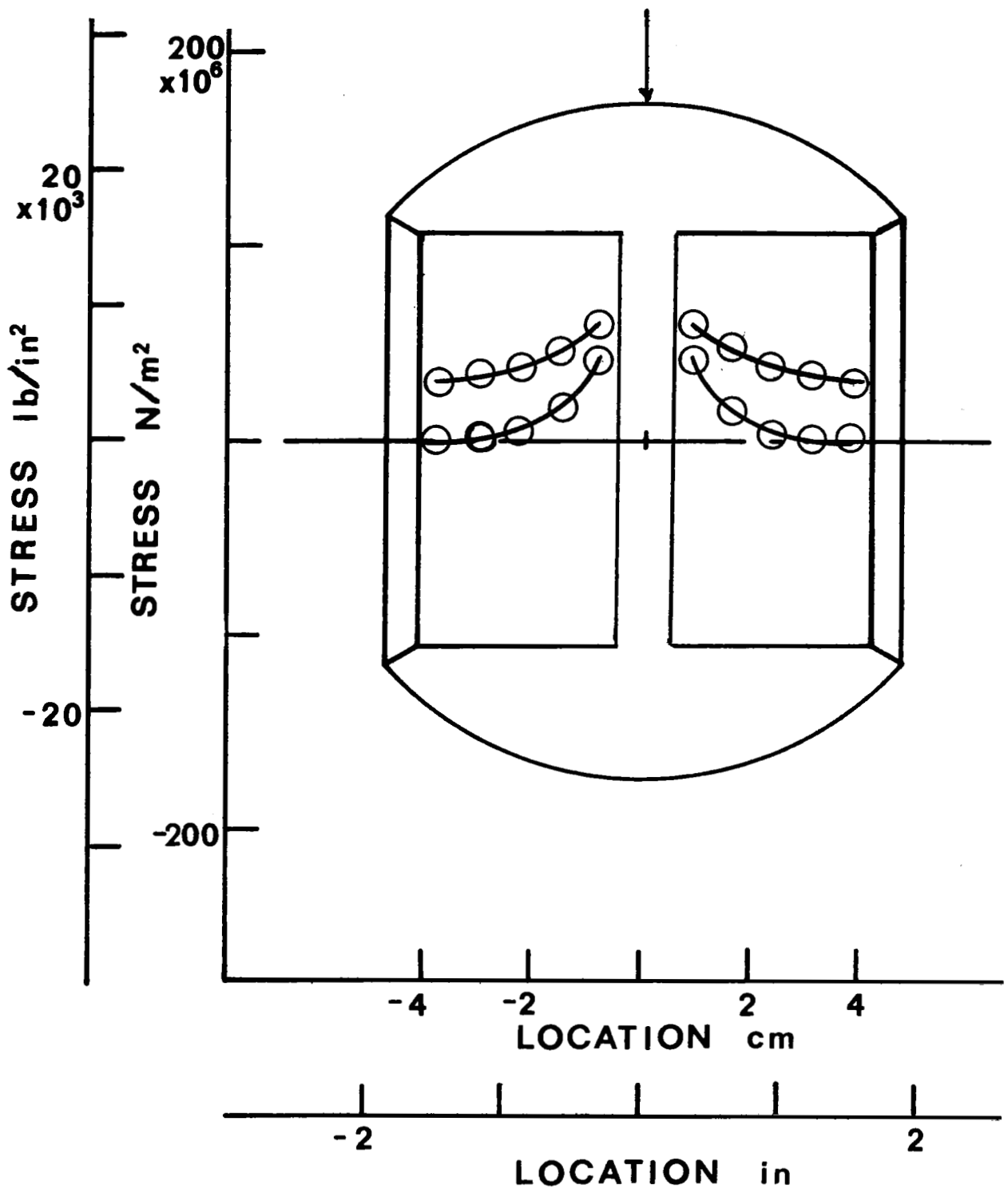


FIGURE 6 a PRINCIPAL STRESSES  $\theta=0$ ,  $\phi=0$

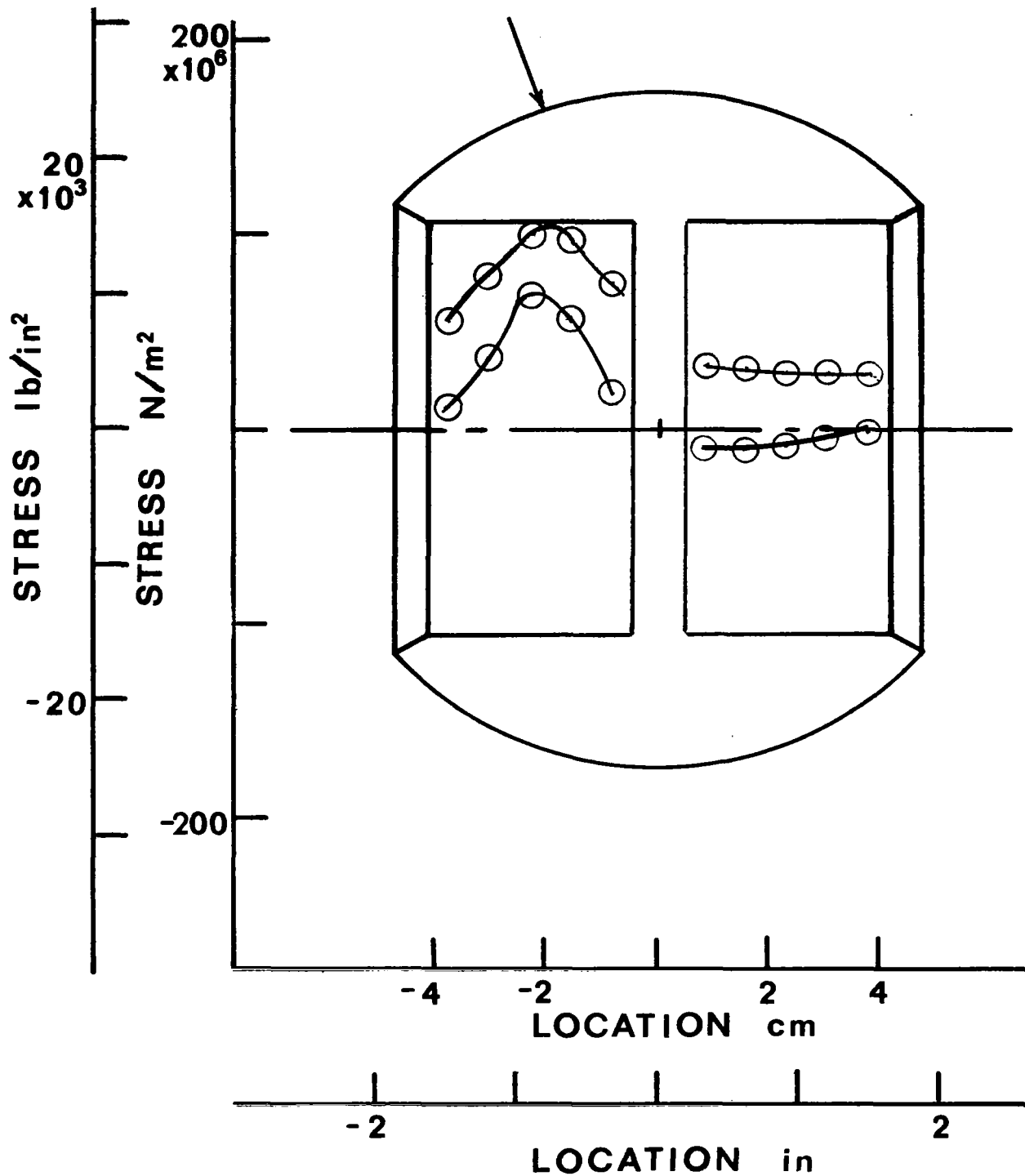


FIGURE 6 b PRINCIPAL STRESSES  $\Theta=0$ ,  $\phi=20$



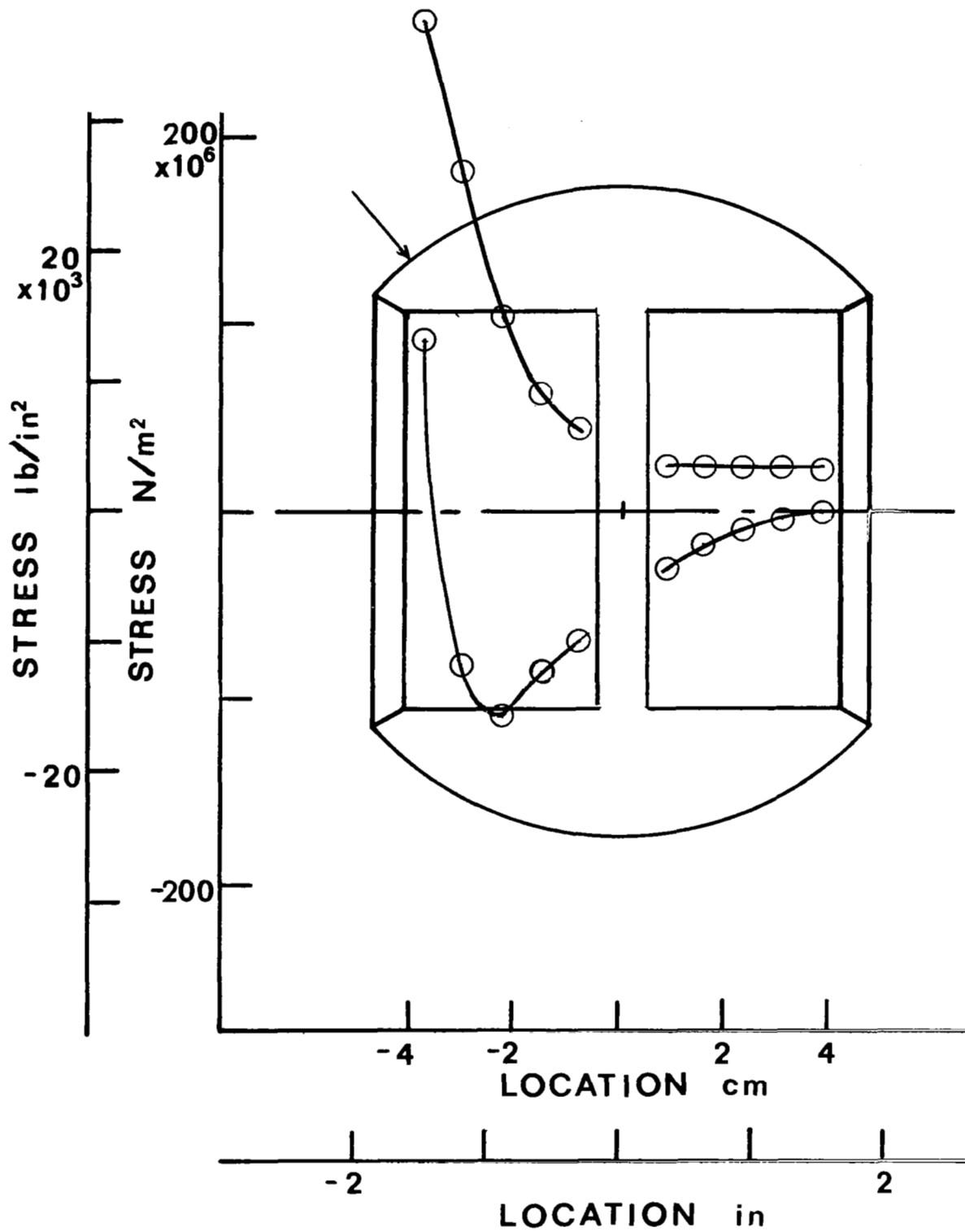


FIGURE 6 c PRINCIPAL STRESSES  $\theta=0$ ,  $\phi=40$

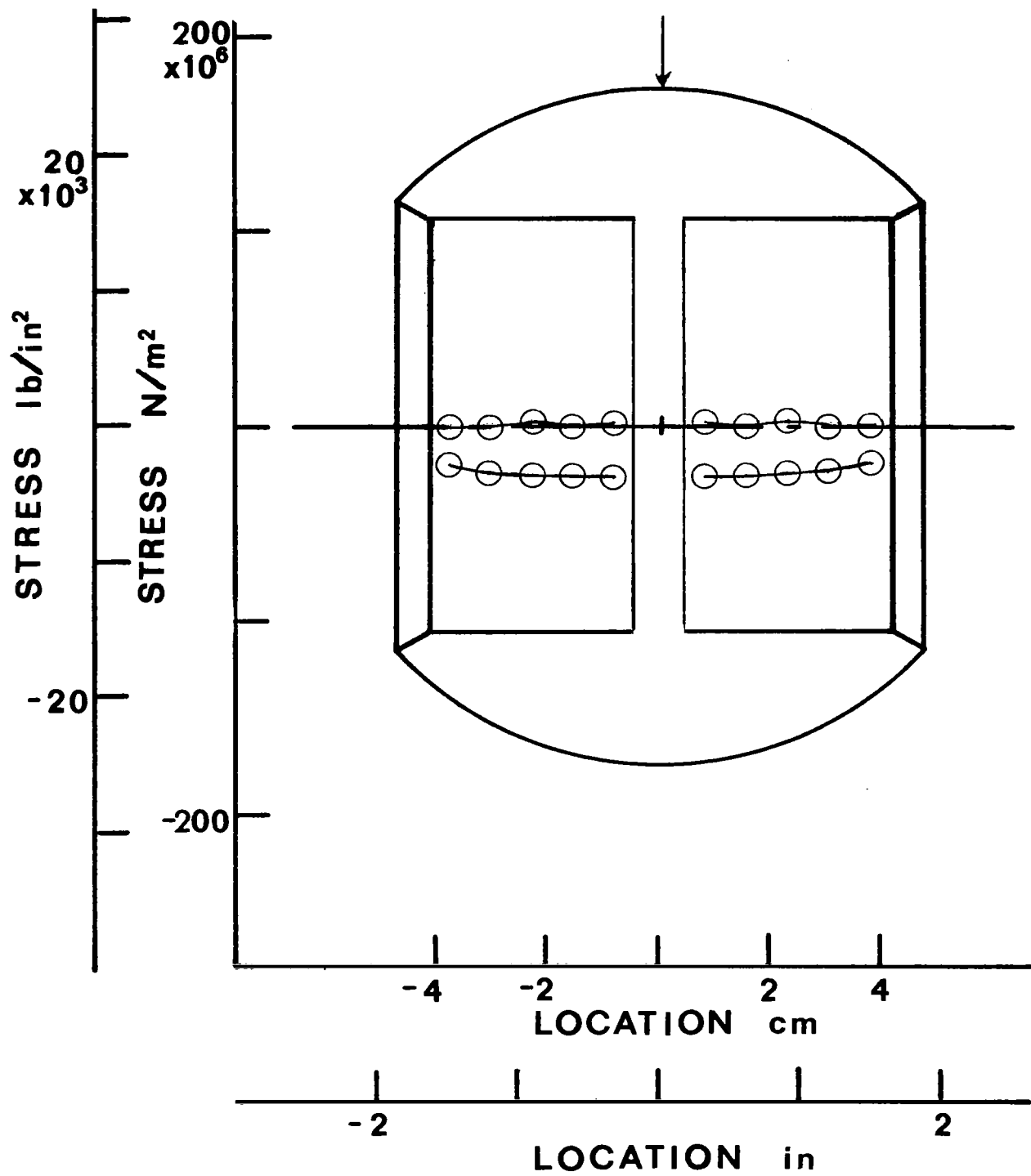


FIGURE 6 d PRINCIPAL STRESSES  $\theta=90$ ,  $\phi=0$

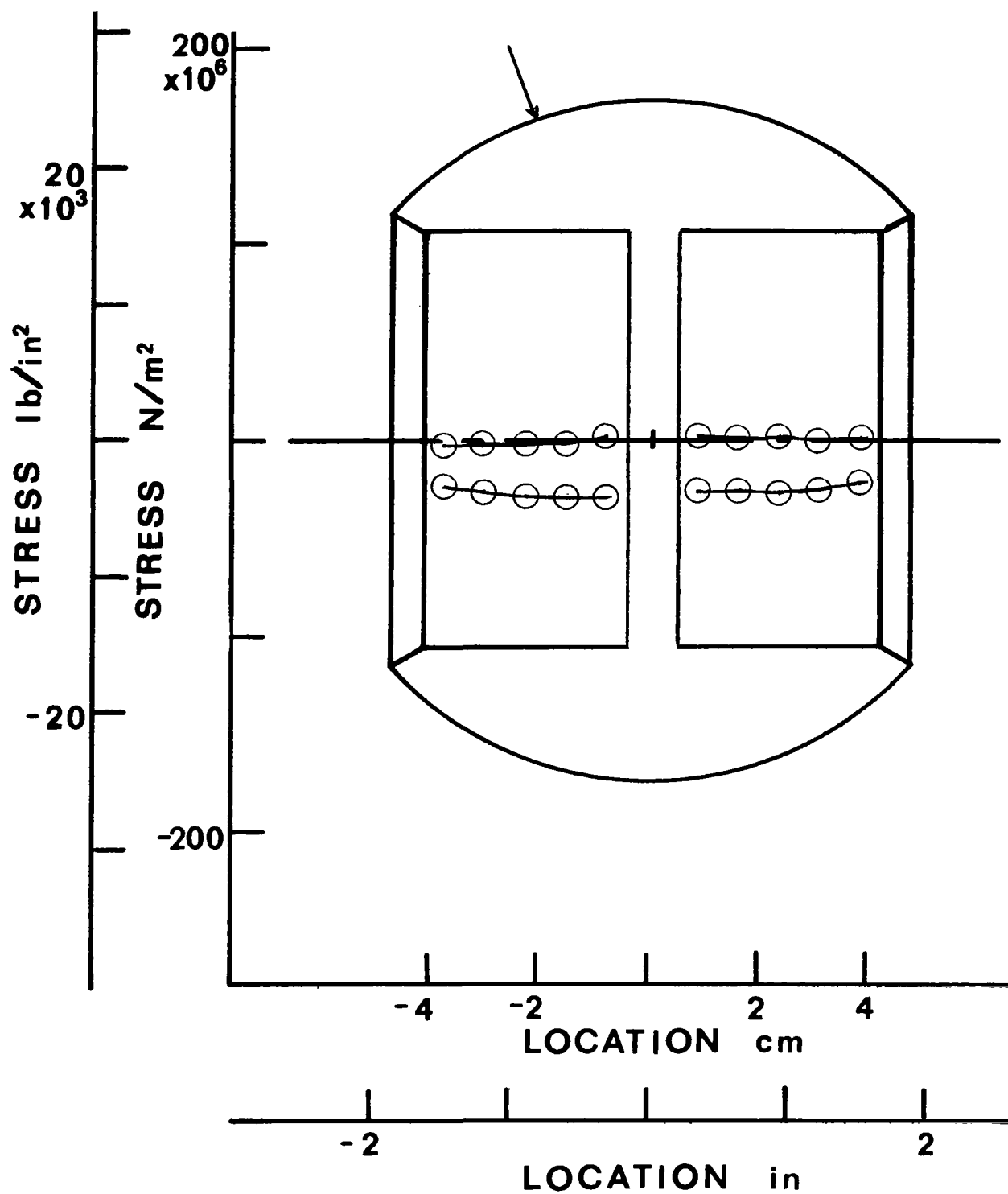


FIGURE 6 e PRINCIPAL STRESSES  $\Theta=90$ ,  $\phi=20$

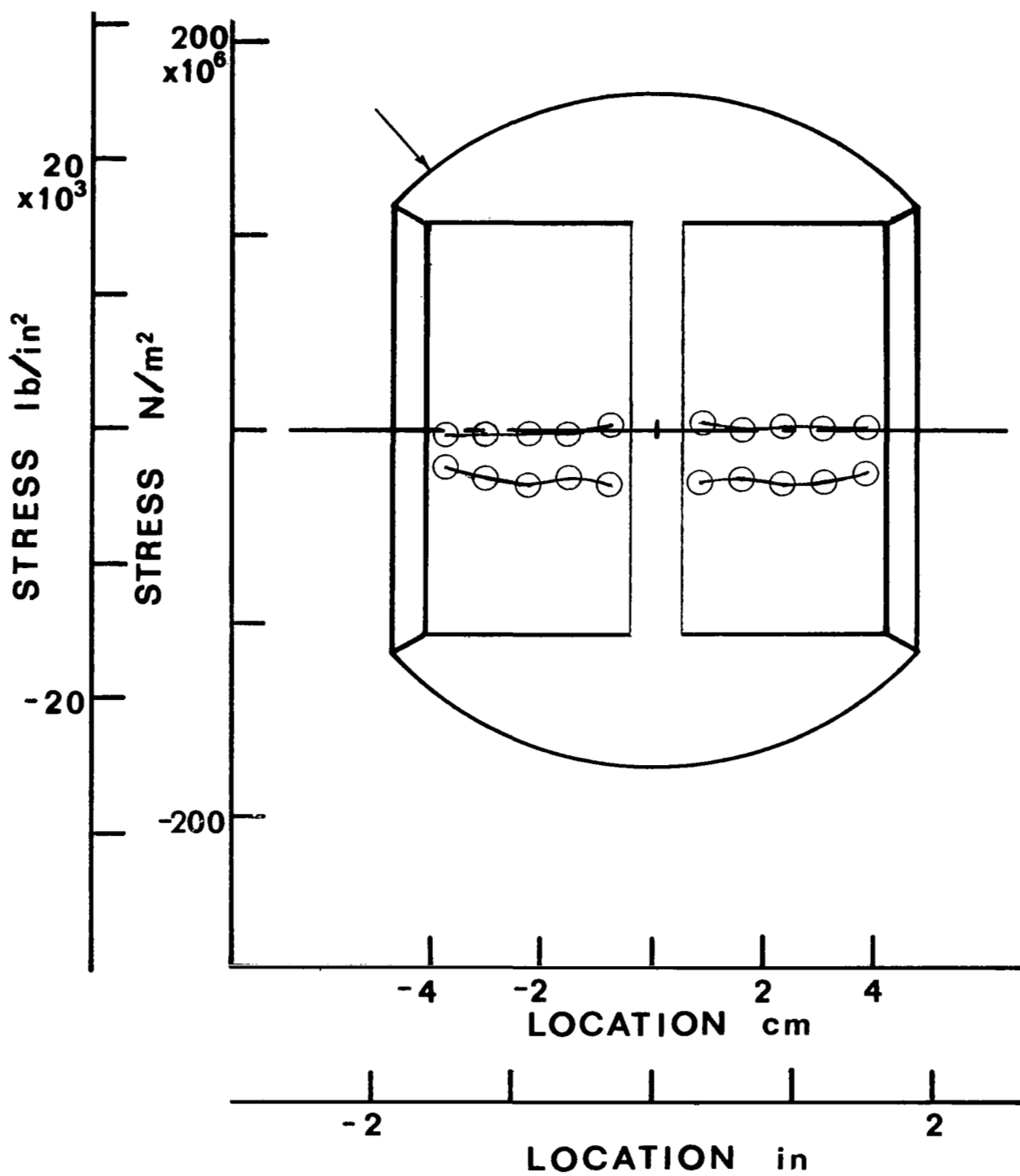


FIGURE 6 f PRINCIPAL STRESSES  $\Theta=90$ ,  $\phi=40$

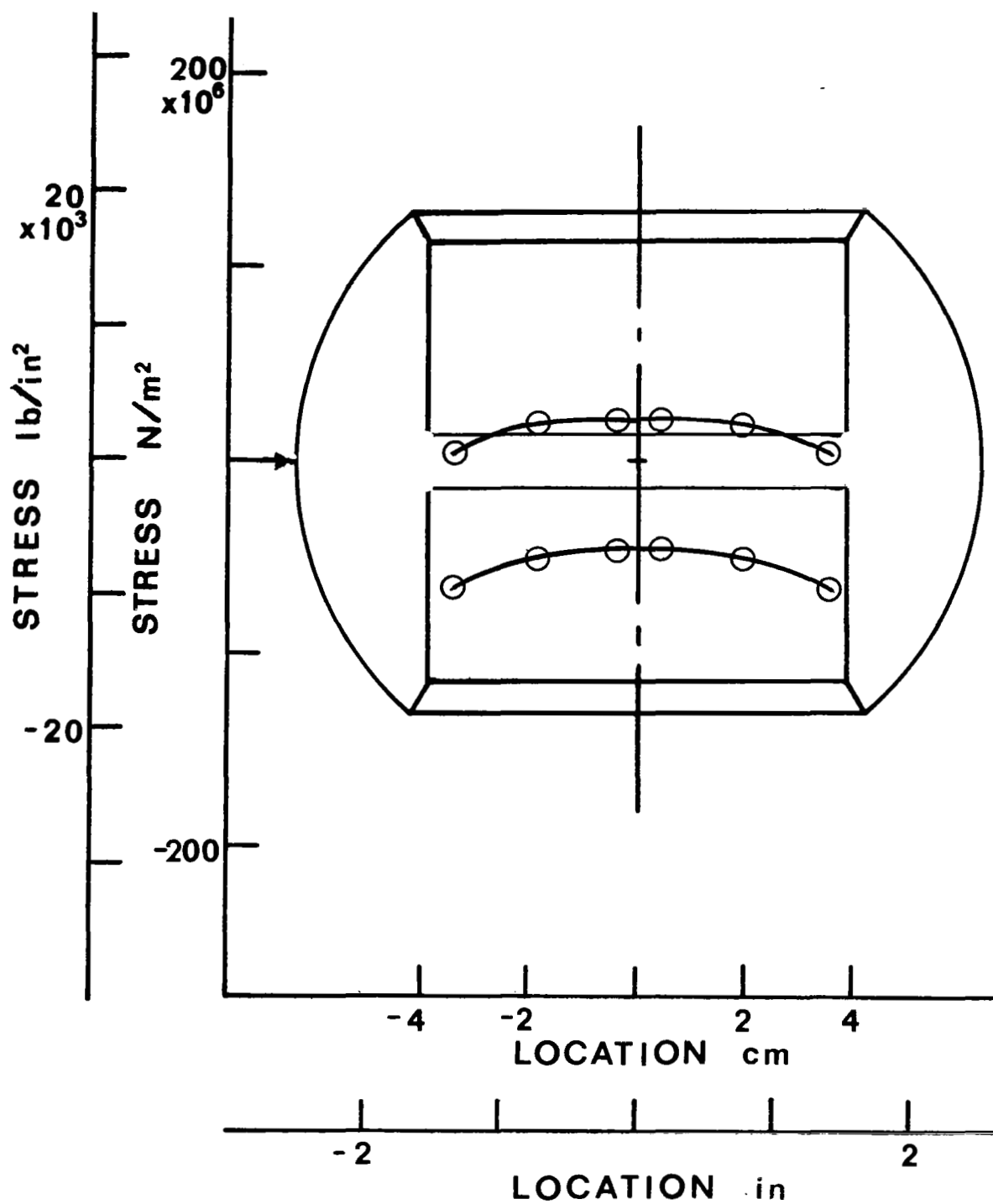


FIGURE 7 a PRINCIPAL STRESSES  $\Theta=0$ ,  $\phi=0$   
WEB

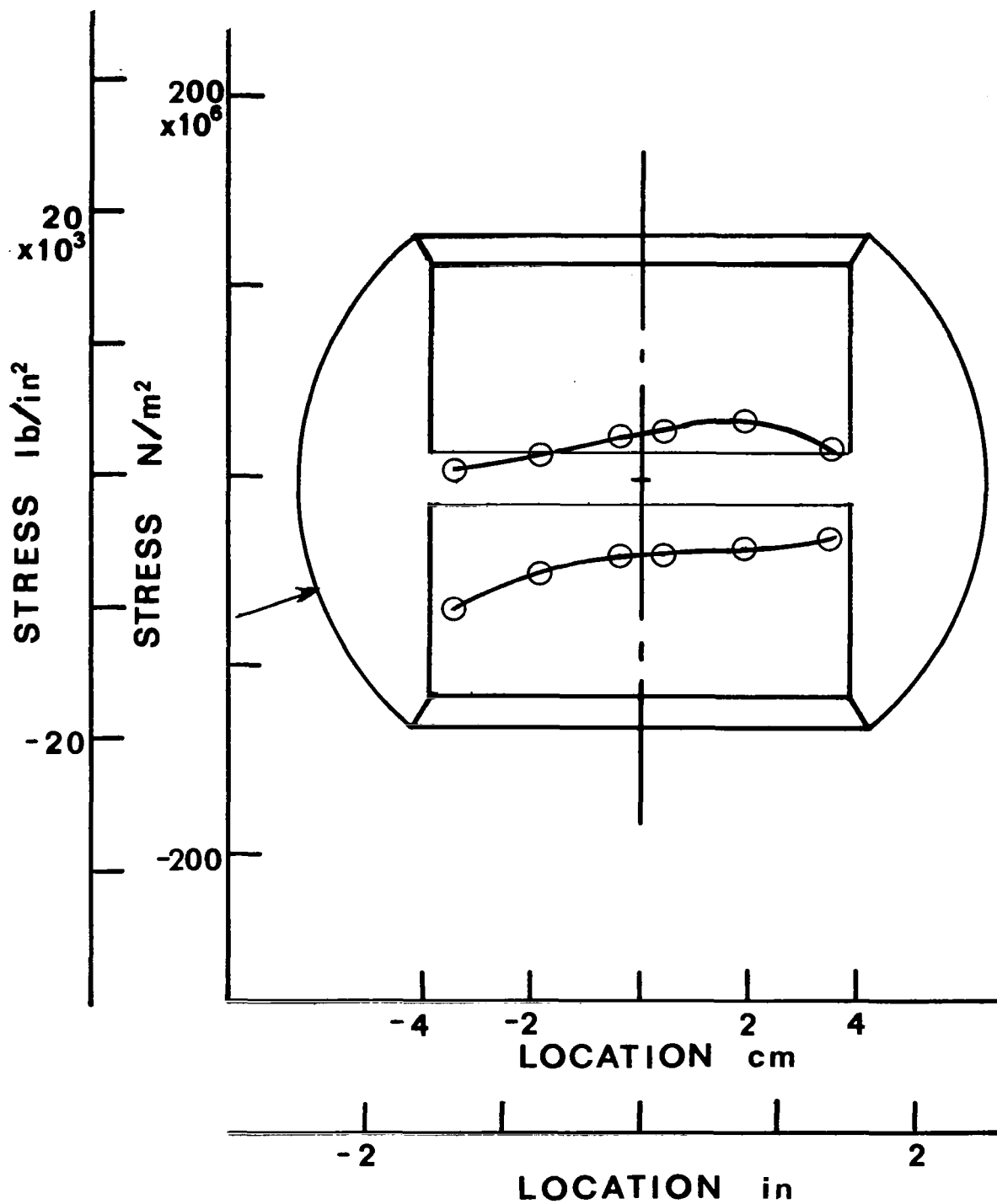


FIGURE 7 b PRINCIPAL STRESSES  $\Theta=0$ ,  $\phi=20$   
WEB

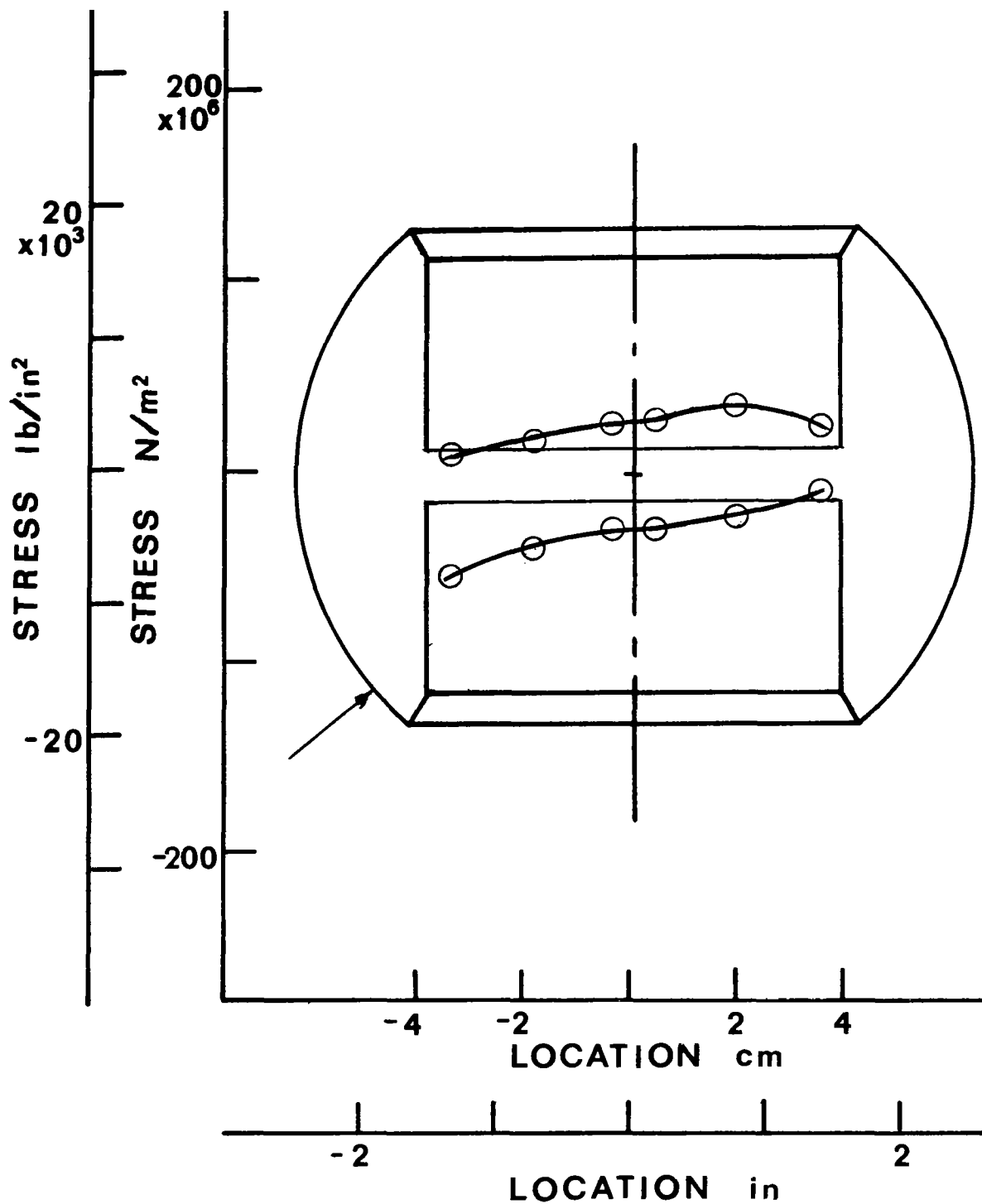


FIGURE 7 c PRINCIPAL STRESSES  $\Theta=0$ ,  $\phi=40$   
WEB

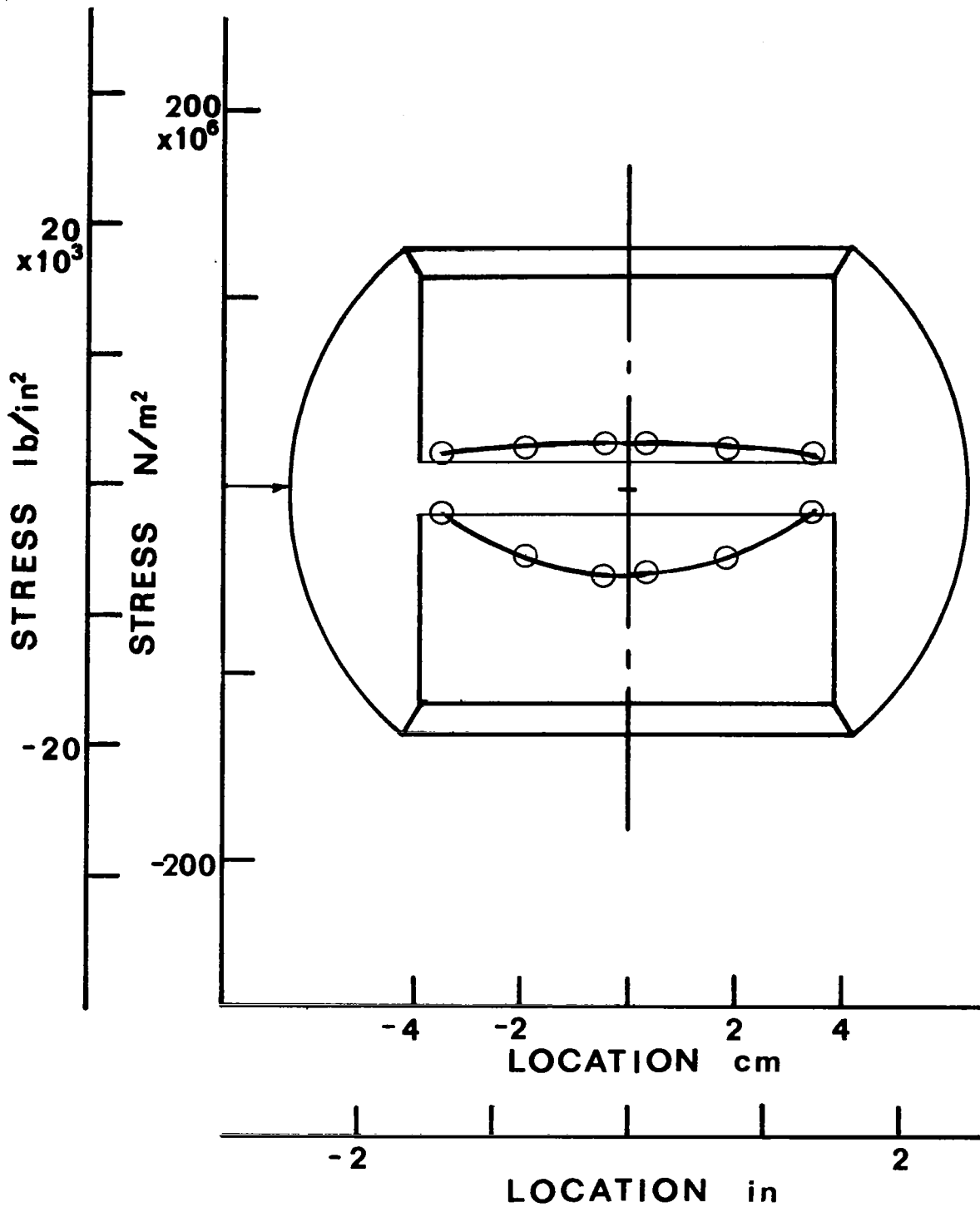


FIGURE 7 d PRINCIPAL STRESSES  $\Theta=90$ ,  $\phi=0$   
WEB



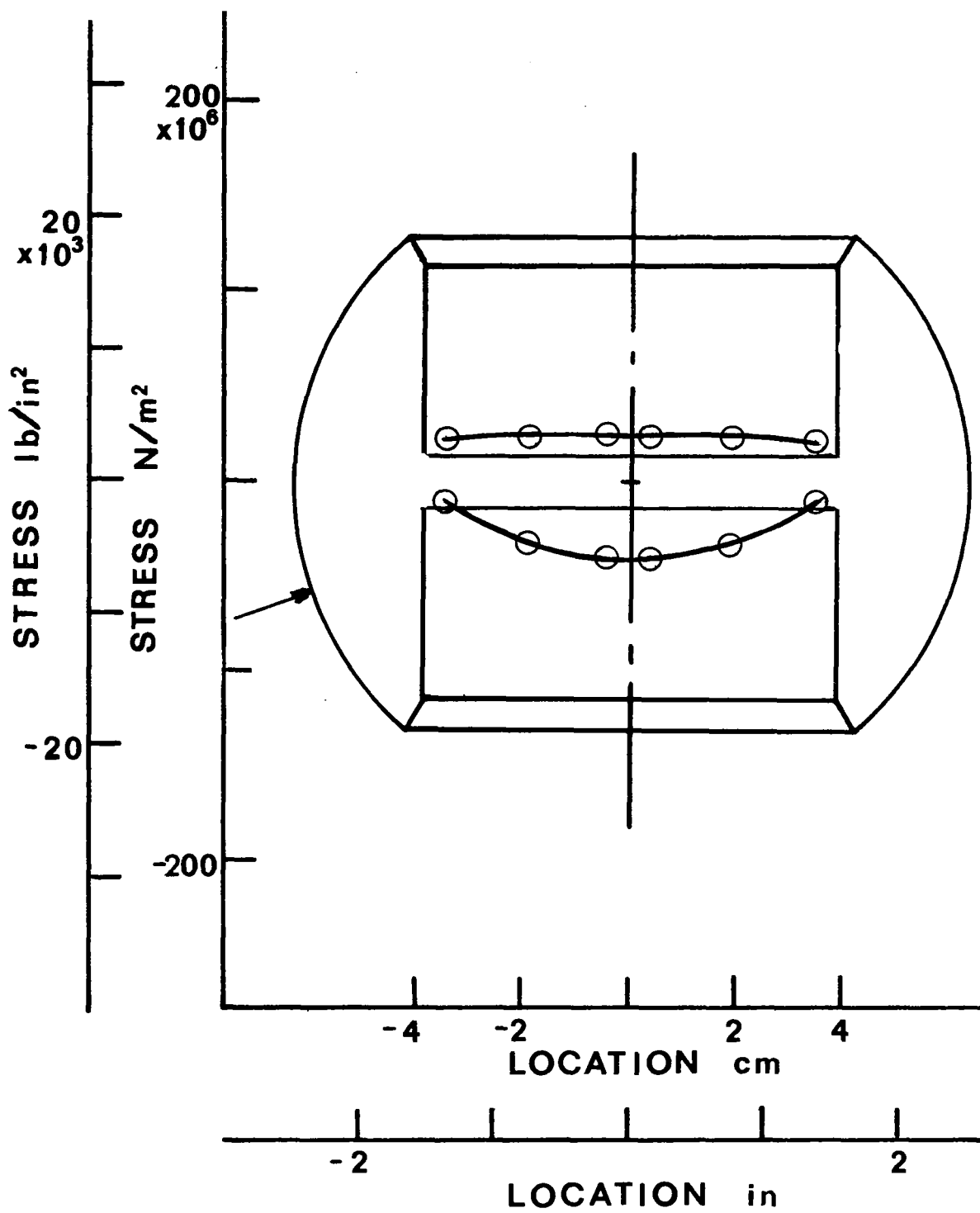


FIGURE 7 e PRINCIPAL STRESSES  $\theta \approx 90$ ,  $\phi = 20$   
WEB

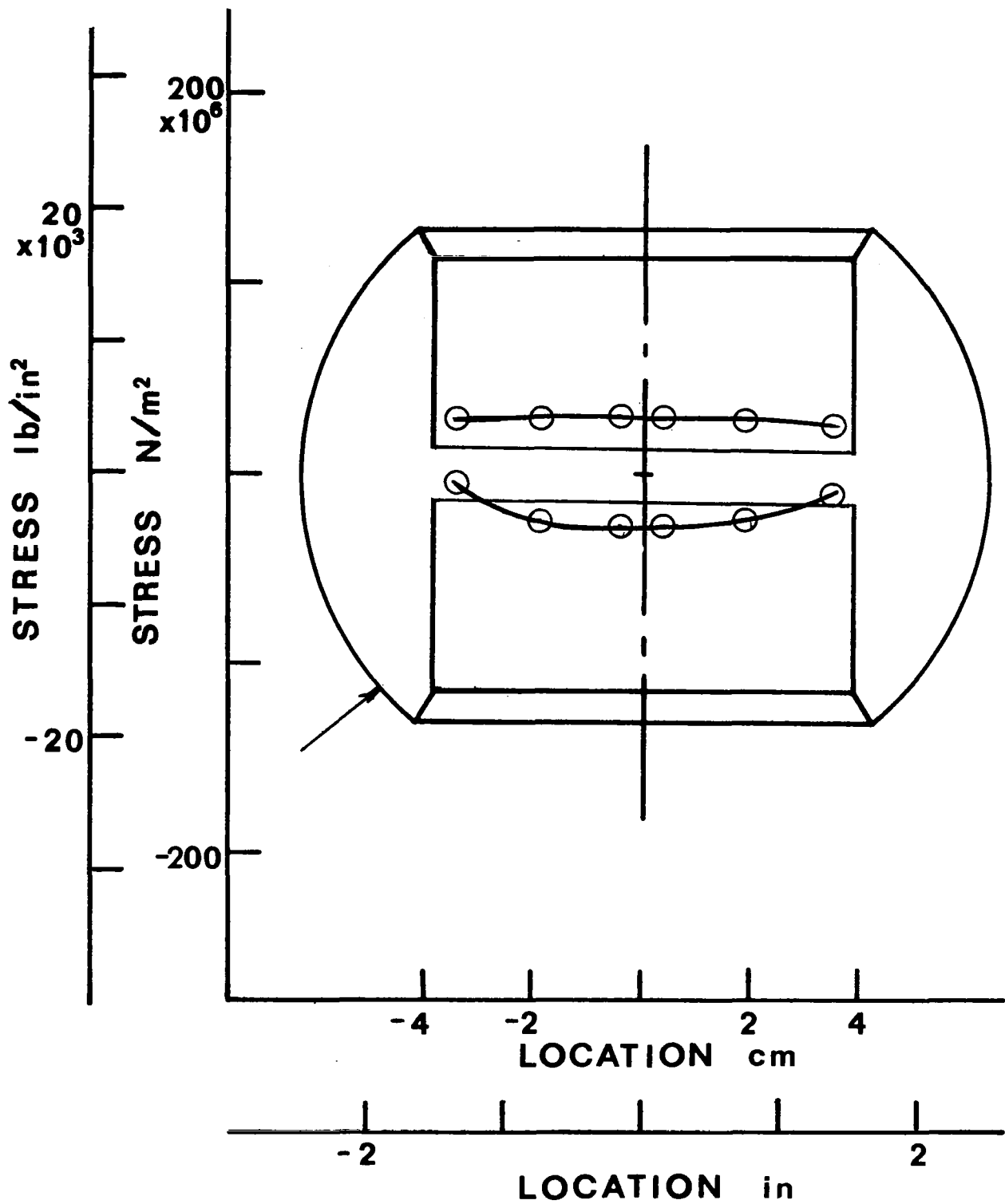


FIGURE 7 f PRINCIPAL STRESSES  $\Theta=90$ ,  $\phi=40$   
WEB

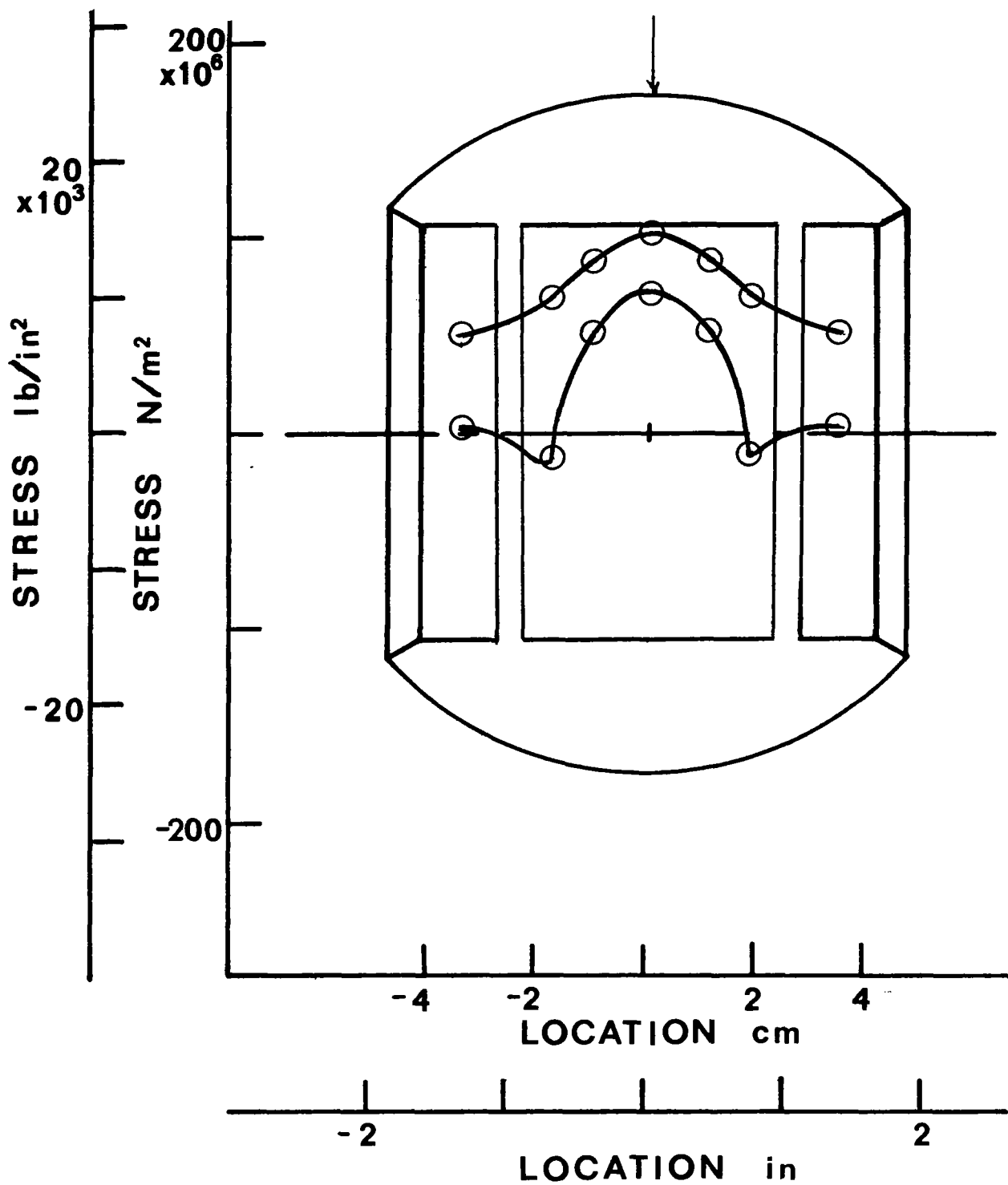


FIGURE 8 a PRINCIPAL STRESSES  $\Theta=0$ ,  $\phi=0$

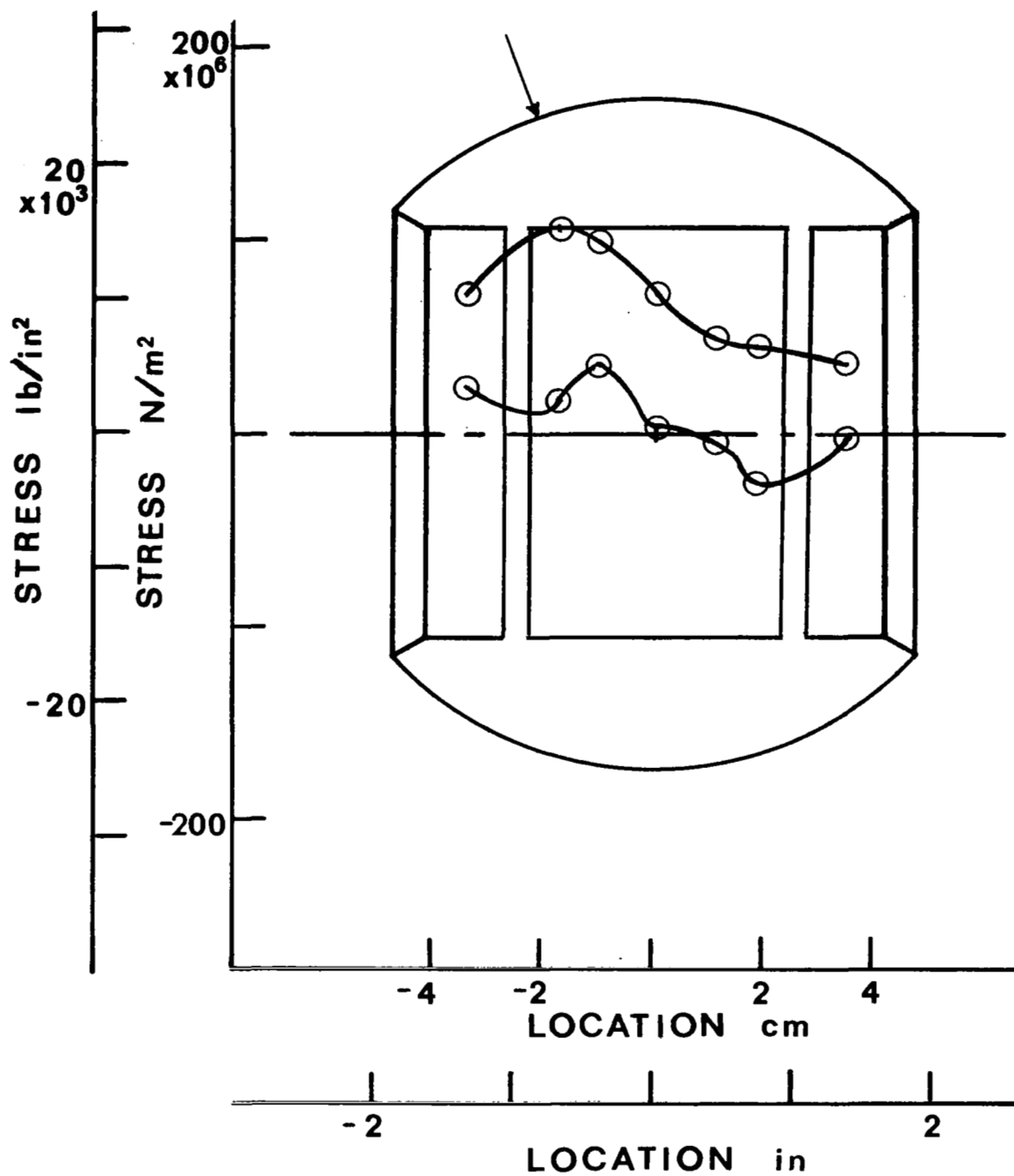


FIGURE 8 b PRINCIPAL STRESSES  $\Theta=0$ ,  $\phi=20$

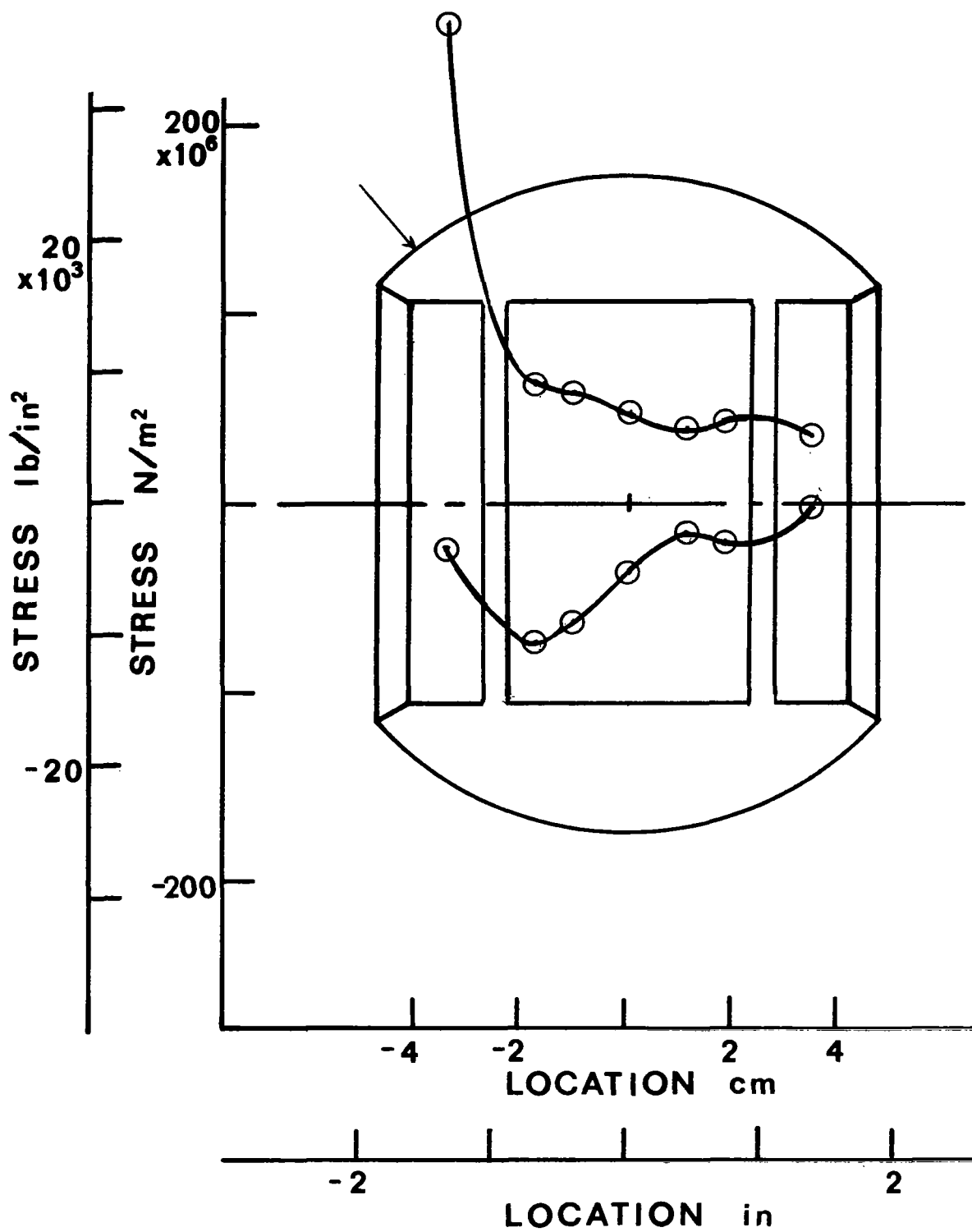


FIGURE 8 c PRINCIPAL STRESSES  $\theta=0$ ,  $\phi=40$

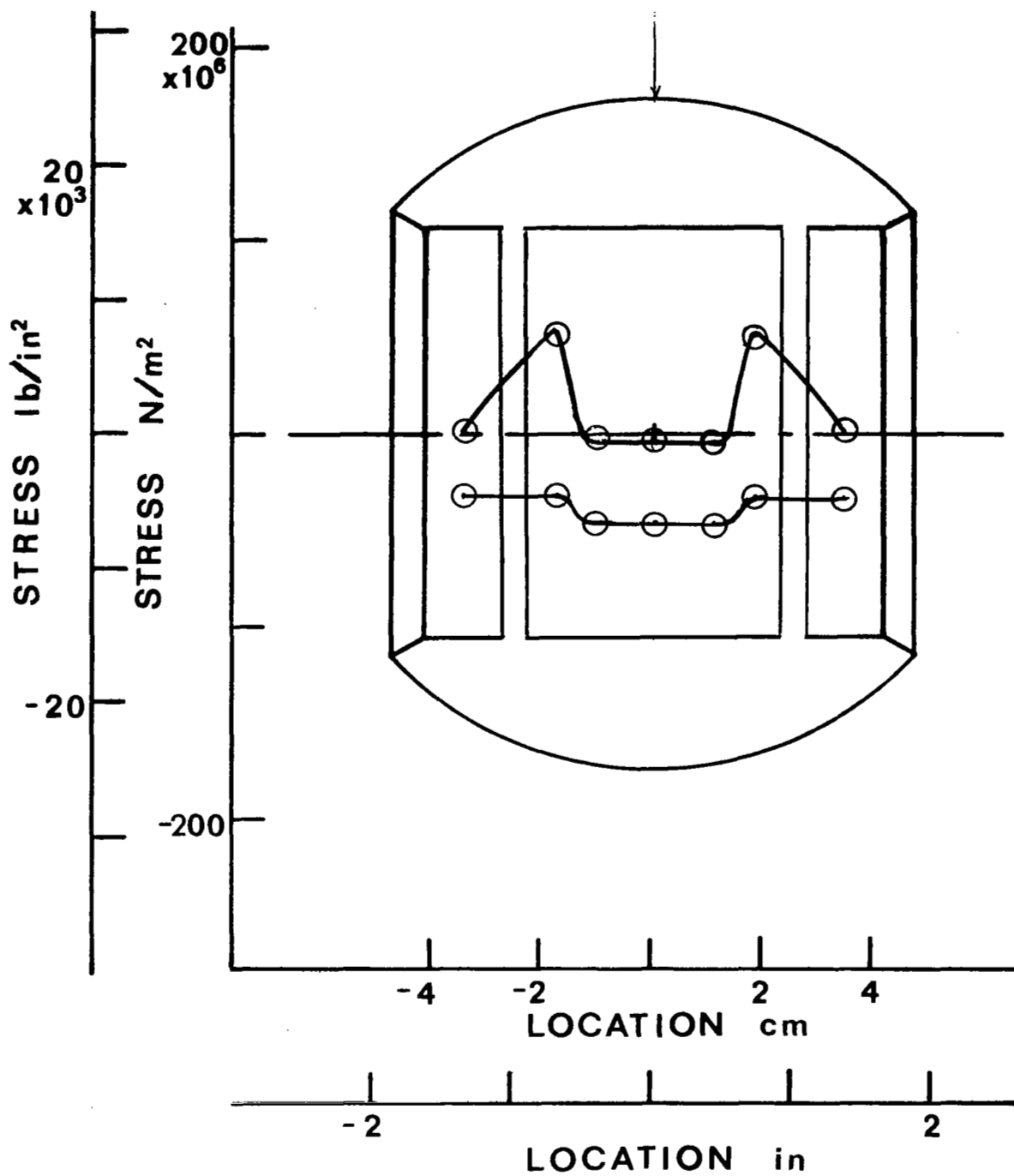


FIGURE 8 d PRINCIPAL STRESSES  $\Theta=90$ ,  $\phi=0$

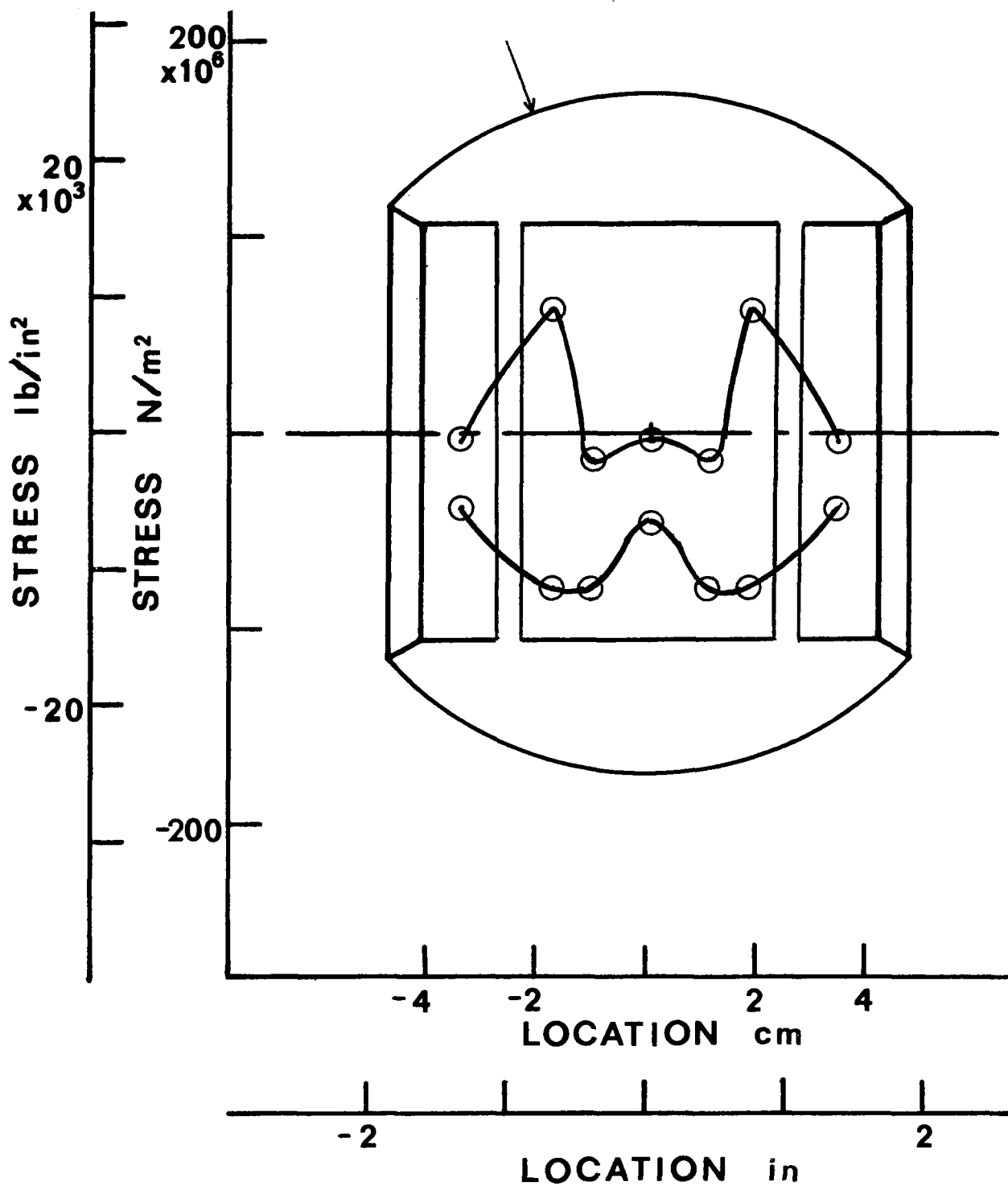


FIGURE 8 e PRINCIPAL STRESSES  $\Theta=90$ ,  $\phi=20$

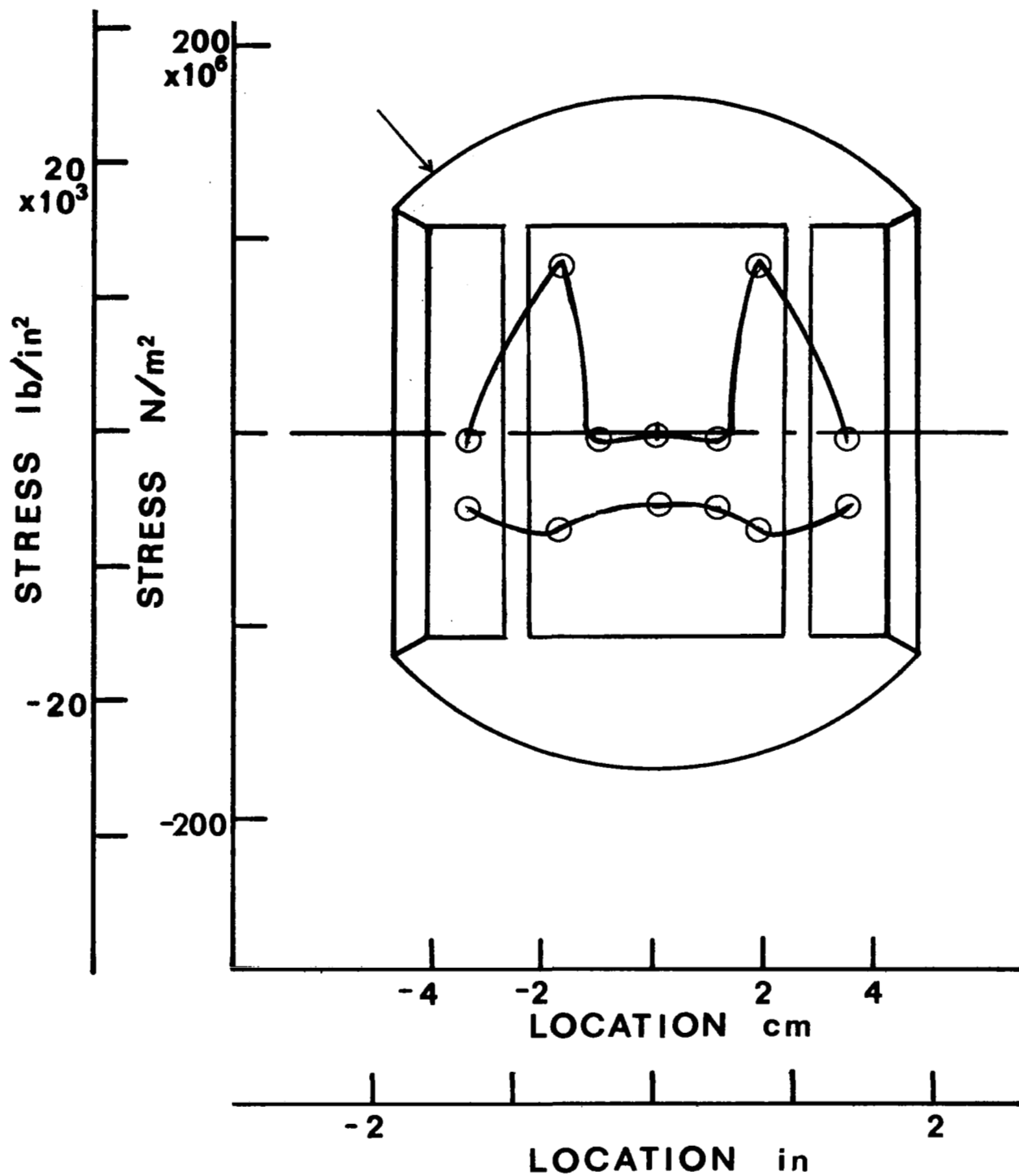


FIGURE 8 f PRINCIPAL STRESSES  $\Theta=90$ ,  $\phi=40$



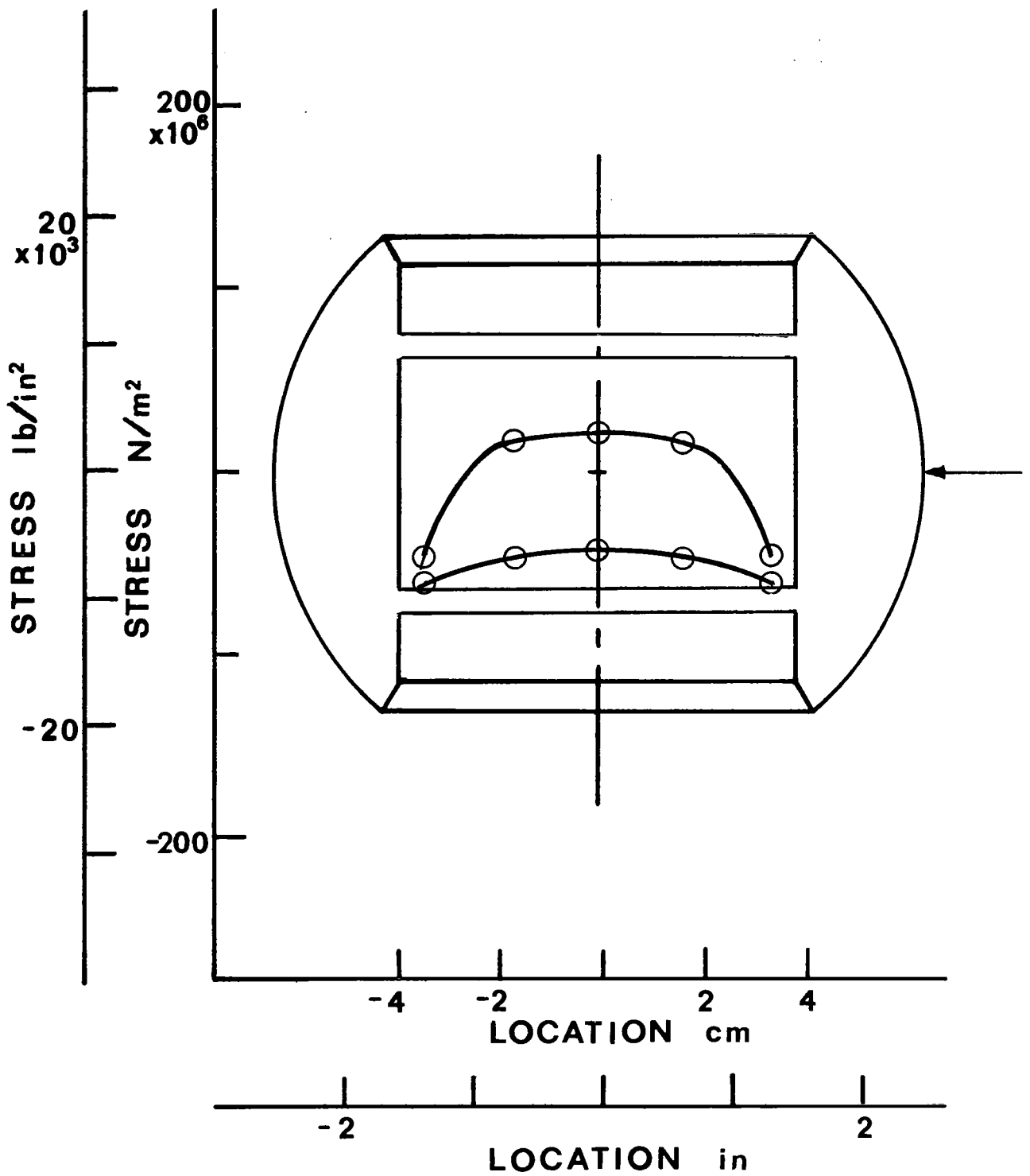


FIGURE 9 a PRINCIPAL STRESSES  $\theta=0$ ,  $\phi=0$   
WEB

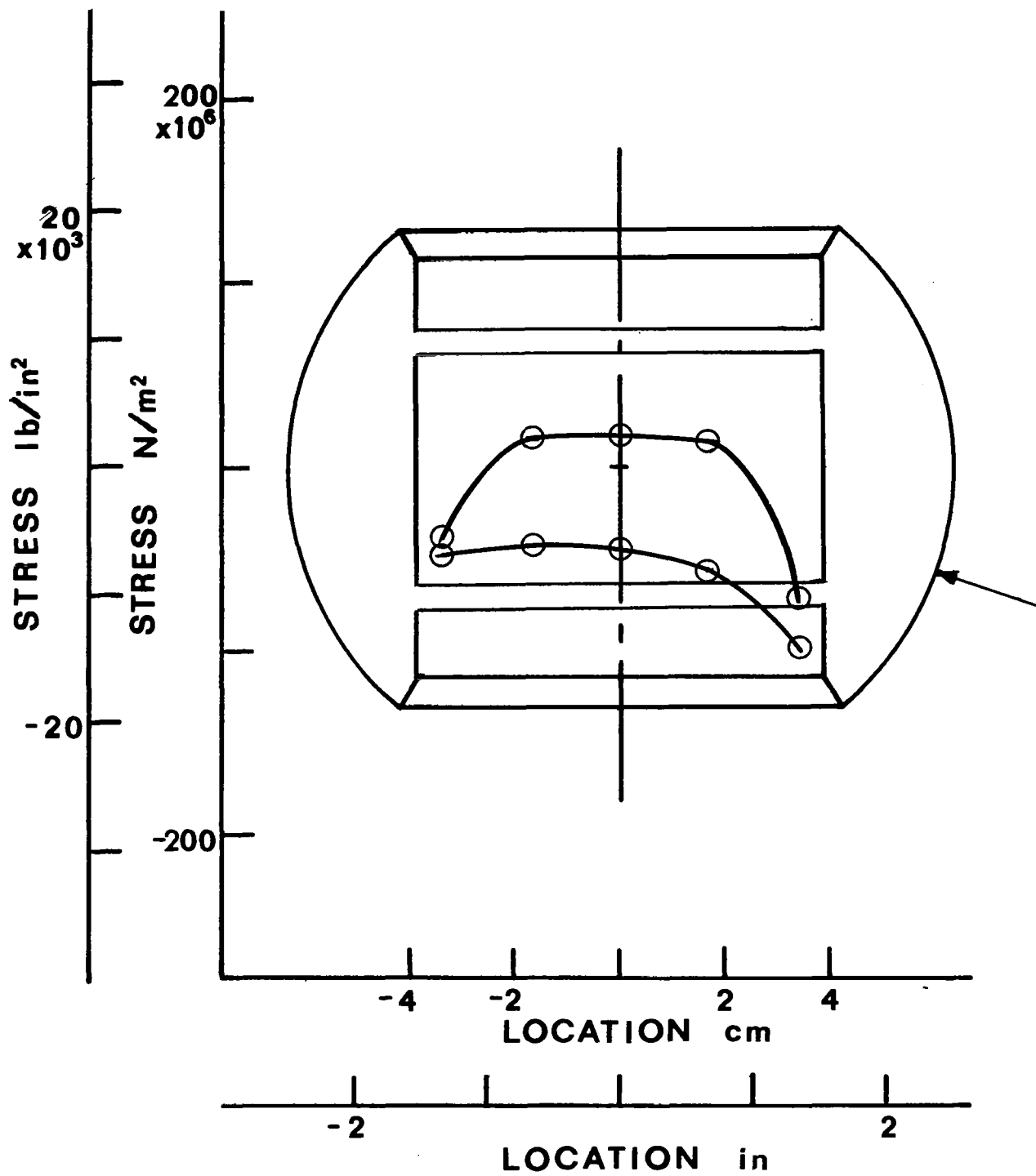


FIGURE 9 b PRINCIPAL STRESSES  $\Theta=0$ ,  $O=20$   
WEB

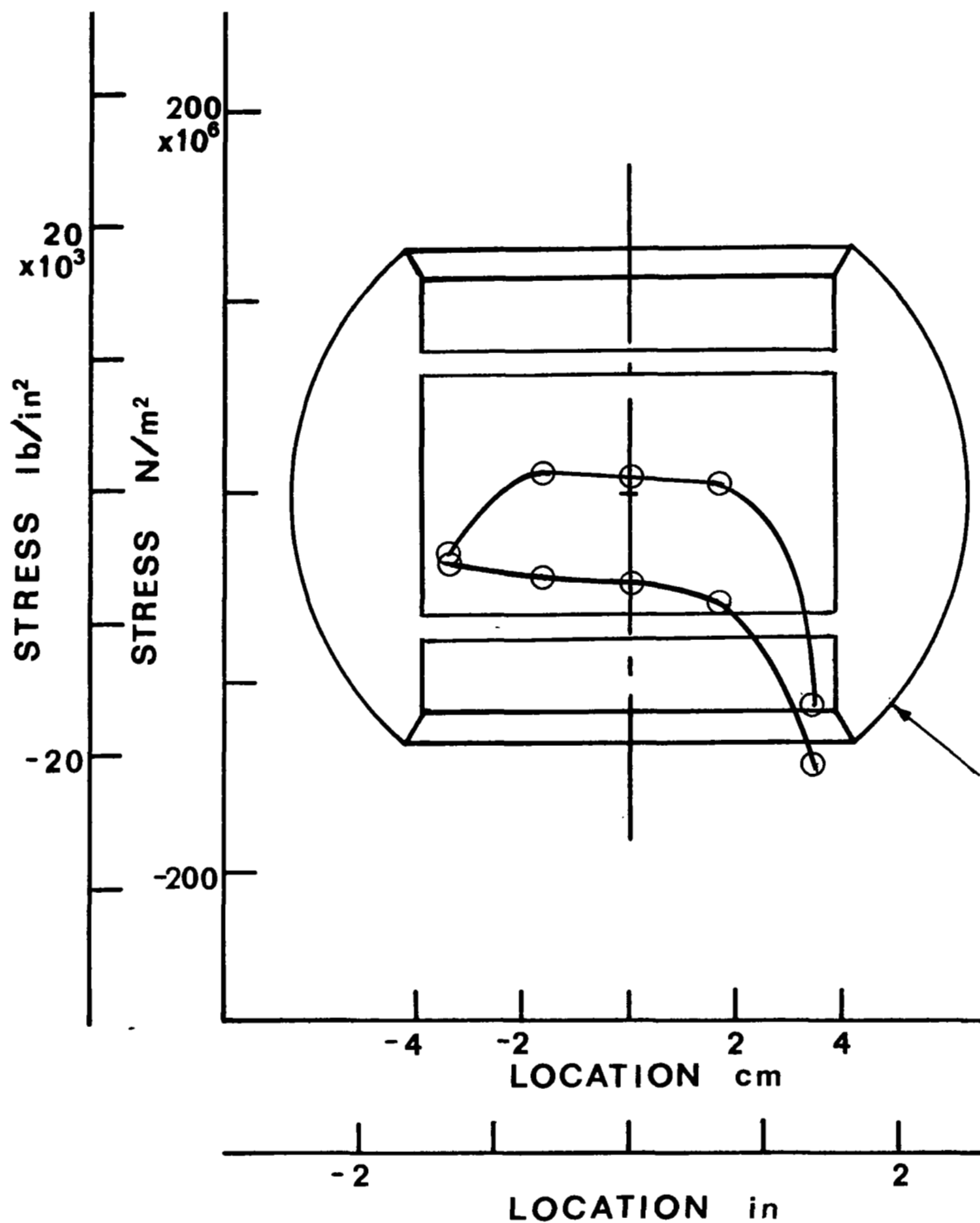


FIGURE 9 c PRINCIPAL STRESSES  $\theta=0$ ,  $\phi=40$   
WEB

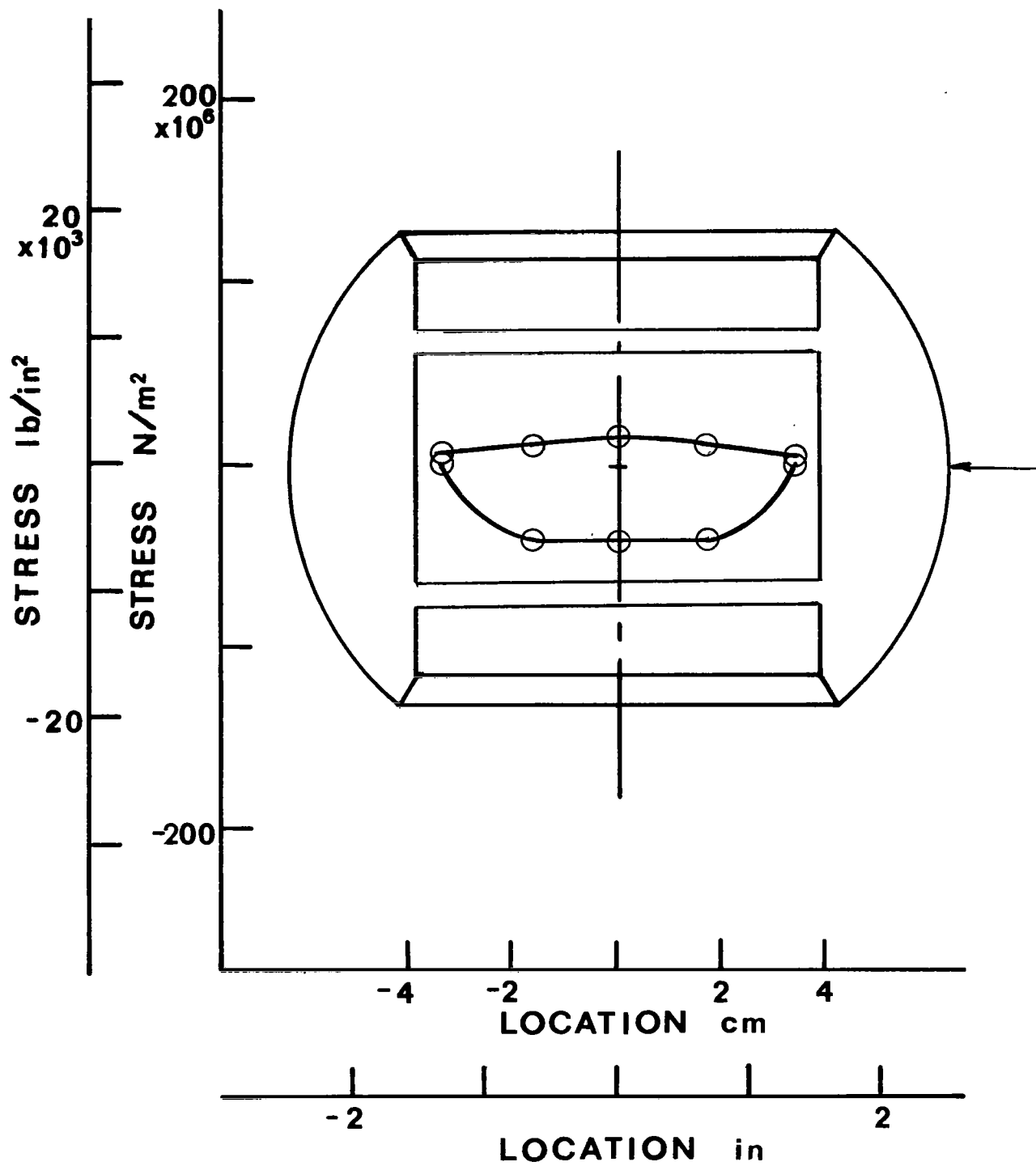


FIGURE 9 d PRINCIPAL STRESSES  $\Theta=90^\circ$ ,  $\phi=0$   
WEB

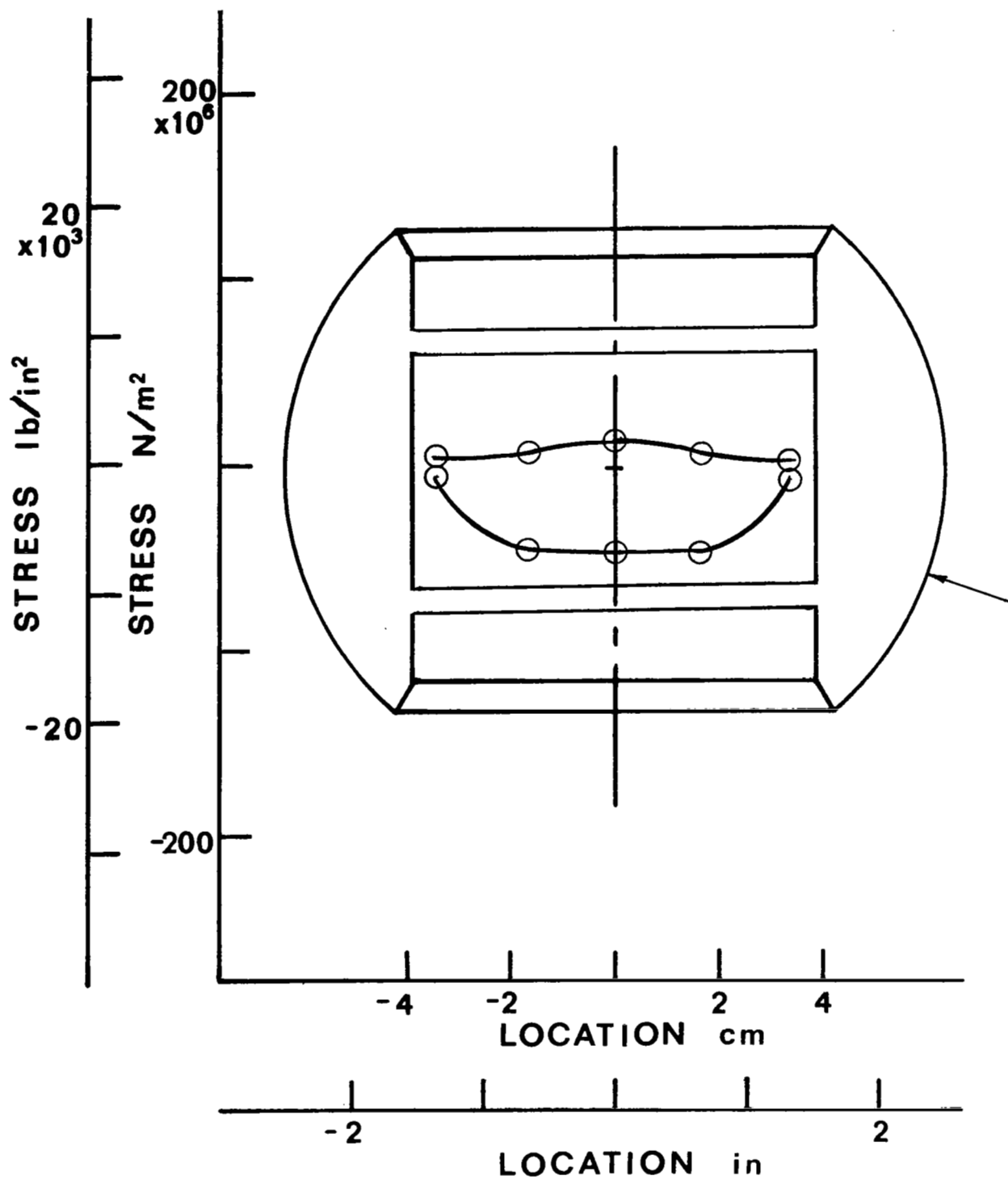


FIGURE 9 e PRINCIPAL STRESSES  $\theta=90$ ,  $\phi=20$   
WEB

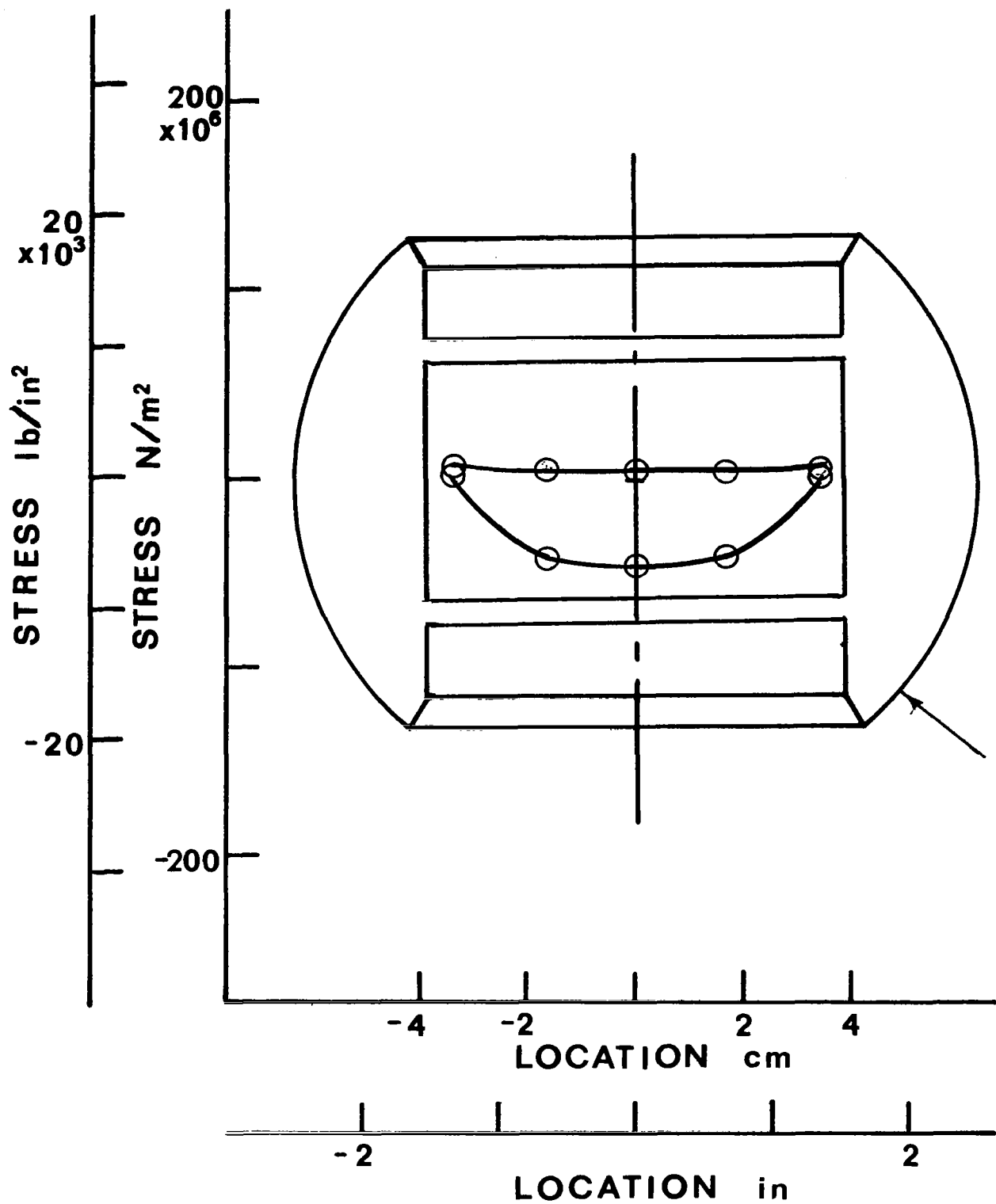


FIGURE 9 f PRINCIPAL STRESSES  $\theta=90$ ,  $\phi=40$   
WEB

TABLE 1

STRAIN GAGE LOCATIONS DISTANCE FROM BALL MIDPLANE TO GAGES

## SINGLE WEBBED MODEL

Interior  
Axial & 45°  
GagesHoop  
Gages

mm	IN	mm	IN
8.4	.33	10.7	.42
15.7	.62	18.0	.71
23.1	.91	25.4	1.00
30.5	1.20	32.8	1.29
37.8	1.49	40.1	1.58

Web  
45° & 90°  
GagesAligned  
Gages

mm	IN	mm	IN
2.3	0.09	0.0	0.00
20.1	0.79	17.8	0.70
38.3	1.51	36.1	1.42

## DOUBLE WEBBED MODEL

Interior  
Axial & 45°  
GagesHoop  
Gages

mm	IN	mm	IN
0.0	0.00	2.3	.09
9.7	.38	11.9	.47
19.3	.76	17.0	.67
35.1	1.38	32.8	1.29

Web  
45° & 90°  
GagesAligned  
Gages

mm	IN	mm	IN
2.3	0.09	0.0	0.00
18.5	0.73	16.3	0.64
36.1	1.42	33.8	1.33

DATA, PRINCIPAL STRAINS, STRESSES, AND ANGLE  
FOR A 44500 N (10000 LB) LOAD ON 127 MM (5 IN) CD  
WEBBED 50 PERCENT MASS REDUCTION MODEL INTERIOR

TABLE 2a

THETA = 0. PHI = 0.

EPSILON A MICRO M/M	EPSILON B MICRO M/M	EPSILON C MICRO M/M	EPSILON 1 MICRO M/M	EPSILON 2 MICRO M/M	SIGMA 1 MN/M*M LB/IN*IN		SIGMA 2 MN/M*M LB/IN*IN		ALPHA DEG
-37.	65.	150.	150.	-37.	31.63	4588.	1.76	255.	-3.
-41.	67.	165.	165.	-41.	34.73	5037.	1.91	277.	-1.
-32.	86.	180.	181.	-33.	38.84	5633.	4.89	710.	-3.
17.	111.	204.	204.	17.	47.53	6893.	17.77	2578.	-0.
119.	181.	231.	231.	119.	60.67	8800.	42.75	6200.	-3.
119.	181.	231.	231.	119.	60.67	8800.	42.75	6200.	-3.
17.	111.	204.	204.	17.	47.53	6893.	17.77	2578.	-0.
-32.	86.	180.	181.	-33.	38.84	5633.	4.89	710.	-3.
-41.	67.	165.	165.	-41.	34.73	5037.	1.91	277.	-1.
-37.	65.	150.	150.	-37.	31.63	4588.	1.76	255.	-3.

THETA = 0. PHI = 20.

EPSILON A MICRO M/M	EPSILON B MICRO M/M	EPSILON C MICRO M/M	EPSILON 1 MICRO M/M	EPSILON 2 MICRO M/M	SIGMA 1 MN/M*M LB/IN*IN		SIGMA 2 MN/M*M LB/IN*IN		ALPHA DEG
-24.	127.	242.	243.	-25.	53.56	7769.	10.85	1574.	-4.
64.	207.	323.	324.	63.	77.89	11298.	36.46	5288.	-3.
185.	297.	382.	383.	184.	99.59	14444.	67.95	9856.	-4.
142.	264.	385.	385.	142.	97.19	14097.	58.53	8489.	-0.
-18.	140.	332.	333.	-19.	74.37	10786.	18.42	2671.	3.
-93.	64.	168.	171.	-96.	32.27	4680.	-10.11	-1466.	-6.
-95.	34.	163.	163.	-95.	30.57	4434.	-10.48	-1520.	0.
-78.	48.	147.	148.	-79.	28.22	4093.	-7.83	-1136.	-3.
-61.	52.	142.	143.	-62.	28.22	4093.	-4.29	-622.	-3.
-39.	56.	133.	133.	-39.	27.05	4019.	0.13	19.	-3.

THETA = 0. PHI = 40.

EPSILON A MICRO M/M	EPSILON B MICRO M/M	EPSILON C MICRO M/M	EPSILON 1 MICRO M/M	EPSILON 2 MICRO M/M	SIGMA 1 MN/M*M LB/IN*IN		SIGMA 2 MN/M*M LB/IN*IN		ALPHA DEG
65.	589.	1124.	1124.	65.	259.92	37698.	91.42	13259.	0.
-641.	92.	982.	986.	-645.	180.10	26121.	-79.34	-11507.	3.
-660.	-63.	642.	644.	-662.	101.28	14689.	-186.60	-15460.	2.
-495.	-37.	422.	422.	-495.	62.17	9016.	-83.74	-12145.	0.
-392.	-45.	302.	302.	-392.	41.91	6079.	-68.51	-9936.	0.
-175.	22.	158.	161.	-178.	24.42	3542.	-29.44	-4271.	-5.
-124.	11.	146.	146.	-124.	24.73	3587.	-18.23	-2644.	0.
-85.	36.	136.	136.	-85.	25.20	3654.	-10.13	-1469.	-3.
-57.	46.	125.	126.	-58.	24.65	3575.	-4.56	-661.	-4.
-31.	48.	112.	112.	-31.	23.41	3395.	0.53	77.	-3.



DATA, PRINCIPAL STRAINS, STRESSES, AND ANGLE  
FOR A 44500 N (10000 LB) LOAD ON 127 MM (5 IN) OD  
WEBBED 50 PERCENT MASS REDUCTION MODEL INTERIOR

TABLE 2b

THETA = 90. PHI = 0.					SIGMA 1		SIGMA 2		ALPHA
EPSILON A	EPSILON B	EPSILON C	EPSILON 1	EPSILON 2	MN/M*M LB/IN*IN		MN/M*M LB/IN*IN		DEG
MICRO M/M	MICRO M/M	MICRO M/M	MICRO M/M	MICRO M/M					
27.	-40.	-94.	27.	-94.	-0.22	-32.	-19.58	-2840.	-3.
32.	-48.	-110.	33.	-111.	-0.14	-20.	-22.91	-3323.	-4.
47.	-43.	-120.	47.	-120.	2.54	368.	-24.11	-3497.	-2.
40.	-42.	-124.	40.	-124.	0.64	92.	-25.46	-3692.	0.
48.	-49.	-128.	48.	-128.	2.26	327.	-25.89	-3756.	-3.
48.	-49.	-128.	48.	-128.	2.26	327.	-25.89	-3756.	-3.
40.	-42.	-124.	40.	-124.	0.64	92.	-25.46	-3692.	0.
47.	-43.	-120.	47.	-120.	2.54	368.	-24.11	-3497.	-2.
32.	-48.	-110.	33.	-111.	-0.14	-20.	-22.91	-3323.	-4.
27.	-40.	-94.	27.	-94.	-0.22	-32.	-19.58	-2840.	-3.

THETA = 90. PHI = 20.					SIGMA 1		SIGMA 2		ALPHA
EPSILON A	EPSILON B	EPSILON C	EPSILON 1	EPSILON 2	MN/M*M LB/IN*IN		MN/M*M LB/IN*IN		DEG
MICRO M/M	MICRO M/M	MICRO M/M	MICRO M/M	MICRO M/M					
26.	-46.	-109.	26.	-109.	-1.50	-217.	-23.03	-3340.	-2.
33.	-43.	-126.	33.	-126.	-1.08	-156.	-26.40	-3829.	1.
38.	-35.	-140.	39.	-141.	-0.68	-99.	-29.46	-4272.	5.
38.	-49.	-136.	38.	-136.	-0.64	-92.	-28.32	-4108.	0.
47.	-14.	-134.	52.	-139.	2.29	332.	-28.00	-4061.	9.
38.	-89.	-121.	51.	-134.	2.47	359.	-27.00	-3916.	-15.
41.	-43.	-126.	41.	-126.	0.73	106.	-25.84	-3748.	-0.
41.	-76.	-125.	48.	-132.	1.86	270.	-26.68	-3870.	-11.
35.	-59.	-118.	37.	-120.	0.22	32.	-24.75	-3590.	-6.
32.	-43.	-99.	33.	-100.	0.63	92.	-20.43	-2963.	-4.

THETA = 90. PHI = 40.					SIGMA 1		SIGMA 2		ALPHA
EPSILON A	EPSILON B	EPSILON C	EPSILON 1	EPSILON 2	MN/M*M LB/IN*IN		MN/M*M LB/IN*IN		DEG
MICRO M/M	MICRO M/M	MICRO M/M	MICRO M/M	MICRO M/M					
19.	-45.	-92.	20.	-93.	-1.85	-269.	-19.72	-2860.	-4.
32.	-36.	-117.	32.	-117.	-0.66	-96.	-24.46	-3547.	2.
27.	-23.	-127.	32.	-132.	-1.79	-260.	-27.76	-4026.	10.
31.	-45.	-120.	31.	-120.	-1.14	-165.	-25.16	-3649.	-0.
42.	8.	-125.	56.	-139.	3.18	461.	-27.71	-4019.	15.
33.	-108.	-111.	61.	-139.	4.34	630.	-27.39	-3973.	-22.
38.	-42.	-122.	38.	-122.	0.32	46.	-25.14	-3646.	0.
35.	-87.	-126.	45.	-136.	0.97	140.	-27.86	-4040.	-14.
38.	-69.	-126.	42.	-130.	0.64	93.	-26.64	-3864.	-8.
36.	-43.	-109.	36.	-109.	0.80	116.	-22.37	-3244.	-3.

DATA, PRINCIPAL STRAINS, STRESSES, AND ANGLE  
FOR A 44500 N (10000 LB) LOAD ON 127 MM (5 IN) OD  
WEBBED 50 PERCENT MASS REDUCTION MODEL WEB

TABLE 2c

THETA = 0. PHI = 0.					SIGMA 1		SIGMA 2		ALPHA
EPSILON A	EPSILON B	EPSILON C	EPSILON 1	EPSILON 2	MN/M**M LB/IN*IN		MN/M**M LB/IN*IN		DEG
MICRO M/M	MICRO M/M	MICRO M/M	MICRO M/M	MICRO M/M					
-331.	-15.	99.	117.	-319.	4.79	695.	-64.48	-9353.	-12.
-263.	-24.	166.	167.	-264.	20.32	2904.	-48.68	-7061.	-3.
-248.	-13.	171.	173.	-250.	22.20	3220.	-44.96	-6520.	-3.
-248.	-13.	171.	173.	-250.	22.20	3220.	-44.96	-6520.	-3.
-263.	-24.	166.	167.	-264.	20.02	2904.	-48.68	-7061.	-3.
-301.	-15.	99.	117.	-319.	4.79	695.	-64.48	-9353.	-12.

THETA = 0. PHI = 23.					SIGMA 1		SIGMA 2		ALPHA
EPSILON A	EPSILON B	EPSILON C	EPSILON 1	EPSILON 2	MN/M**M LB/IN*IN		MN/M**M LB/IN*IN		DEG
MICRO M/M	MICRO M/M	MICRO M/M	MICRO M/M	MICRO M/M					
-331.	-62.	122.	126.	-335.	5.79	840.	-67.55	-9797.	-5.
-255.	-41.	135.	136.	-256.	13.44	1950.	-48.90	-7093.	-3.
-230.	-5.	168.	169.	-221.	23.37	3389.	-38.73	-5617.	-3.
-224.	-4.	178.	179.	-225.	25.33	3673.	-38.92	-5645.	-3.
-212.	11.	200.	201.	-213.	31.12	4513.	-34.66	-5027.	-2.
-125.	76.	84.	122.	-163.	16.57	2404.	-28.69	-4161.	-21.

THETA = 3. PHI = 40.					SIGMA 1		SIGMA 2		ALPHA
EPSILON A	EPSILON B	EPSILON C	EPSILON 1	EPSILON 2	MN/M**M LB/IN*IN		MN/M**M LB/IN*IN		DEG
MICRO M/M	MICRO M/M	MICRO M/M	MICRO M/M	MICRO M/M					
-264.	-32.	126.	129.	-267.	11.19	1623.	-51.97	-7537.	-5.
-239.	-22.	147.	147.	-209.	19.20	2784.	-37.52	-5442.	-1.
-174.	10.	175.	175.	-174.	27.95	4054.	-27.66	-4011.	-2.
-176.	15.	183.	183.	-176.	29.65	4301.	-27.58	-4001.	-2.
-151.	38.	206.	206.	-151.	36.58	5305.	-20.32	-2948.	-2.
-31.	111.	90.	131.	-72.	24.87	3607.	-7.43	-1078.	-27.

DATA, PRINCIPAL STRAINS, STRESSES, AND ANGLE  
FOR A 44500 N (10000 LB) LOAD ON 127 MM (5 IN) CD  
WEBBED 50 PERCENT MASS REDUCTION MODEL WEB

TABLE 2d

THETA = 90. PHI = 0.					SIGMA 1		SIGMA 2		ALPHA
EPSILON A	EPSILON B	EPSILON C	EPSILON 1	EPSILON 2	MN/M*M LB/IN*IN		MN/M*M LB/IN*IN		DEG
MICRO M/M	MICRO M/M	MICRO M/M	MICRO M/M	MICRO M/M					
101.	-26.	-80.	108.	-87.	18.63	2702.	-12.42	-1802.	-11.
156.	-17.	-205.	156.	-205.	21.50	3119.	-35.98	-5219.	1.
179.	-24.	-248.	179.	-248.	23.82	3454.	-44.21	-6411.	1.
179.	-24.	-248.	179.	-248.	23.82	3454.	-44.21	-6411.	1.
156.	-17.	-205.	156.	-205.	21.50	3119.	-35.98	-5219.	1.
101.	-26.	-80.	108.	-87.	18.63	2702.	-12.42	-1802.	-11.

THETA = 90. PHI = 20.					SIGMA 1		SIGMA 2		ALPHA
EPSILON A	EPSILON B	EPSILON C	EPSILON 1	EPSILON 2	MN/M*M LB/IN*IN		MN/M*M LB/IN*IN		DEG
MICRO M/M	MICRO M/M	MICRO M/M	MICRO M/M	MICRO M/M					
119.	-2.	-74.	122.	-77.	22.49	3262.	-9.19	-1333.	-7.
165.	2.	-191.	166.	-192.	24.58	3565.	-32.26	-4679.	2.
179.	-26.	-221.	179.	-221.	25.63	3717.	-38.04	-5517.	-1.
173.	-10.	-216.	173.	-216.	24.65	3575.	-37.35	-5418.	2.
165.	-25.	-192.	165.	-192.	24.47	3549.	-32.45	-4706.	-2.
113.	-42.	-81.	129.	-97.	22.71	3294.	-13.25	-1922.	-15.

THETA = 90. PHI = 40.					SIGMA 1		SIGMA 2		ALPHA
EPSILON A	EPSILON B	EPSILON C	EPSILON 1	EPSILON 2	MN/M*M LB/IN*IN		MN/M*M LB/IN*IN		DEG
MICRO M/M	MICRO M/M	MICRO M/M	MICRO M/M	MICRO M/M					
137.	23.	-64.	138.	-65.	26.92	3904.	-5.35	-776.	-4.
174.	30.	-157.	175.	-158.	29.07	4216.	-24.04	-3487.	4.
183.	3.	-176.	183.	-176.	29.59	4292.	-27.53	-3992.	-0.
174.	5.	-174.	174.	-174.	27.70	4017.	-27.70	-4017.	1.
168.	-12.	-156.	169.	-157.	27.71	4019.	-24.16	-3504.	-3.
133.	-31.	-76.	149.	-92.	27.55	3996.	-10.71	-1554.	-15.

DATA, PRINCIPAL STRAINS, STRESSES, AND ANGLE  
FOR A 44500 N (10000 LB) LOAD ON 127 MM (5 IN) OD  
DOUBLE WEBBED 50 PERCENT MASS REDUCTION MODEL INTERIOR

TABLE 2e

THETA = 0. PHI = 0.					SIGMA 1		SIGMA 2		ALPHA
EPSILON A	EPSILON B	EPSILON C	EPSILON 1	EPSILON 2	MN/M*M LB/IN*IN		MN/M*M LB/IN*IN		DEG
MICRO M/M	MICRO M/M	MICRO M/M	MICRO M/M	MICRO M/M					
244.	95.	-54.	244.	-54.	51.78	7510.	4.36	633.	0.
286.	-70.	-86.	352.	-152.	69.64	10101.	-10.54	-1529.	-21.
348.	218.	126.	350.	124.	87.95	12756.	52.11	7558.	-5.
388.	290.	210.	388.	210.	102.59	14879.	74.12	10750.	-3.
348.	218.	126.	350.	124.	87.95	12756.	52.11	7558.	-5.
286.	-70.	-86.	352.	-152.	69.64	10101.	-10.54	-1529.	-21.
244.	95.	-54.	244.	-54.	51.78	7510.	4.36	633.	0.

THETA = 0. PHI = 20.					SIGMA 1		SIGMA 2		ALPHA
EPSILON A	EPSILON B	EPSILON C	EPSILON 1	EPSILON 2	MN/M*M LB/IN*IN		MN/M*M LB/IN*IN		DEG
MICRO M/M	MICRO M/M	MICRO M/M	MICRO M/M	MICRO M/M					
320.	168.	16.	320.	16.	73.83	10708.	25.46	3692.	0.
404.	8.	10.	487.	-73.	105.72	15333.	16.61	2409.	-23.
424.	202.	36.	426.	34.	99.15	14380.	36.78	5334.	-4.
342.	98.	-82.	344.	-84.	72.53	10519.	4.30	624.	-4.
244.	74.	-88.	244.	-88.	49.47	7175.	-3.37	-489.	-1.
208.	-96.	-134.	254.	-180.	45.40	6585.	-23.54	-3414.	-19.
180.	60.	-60.	180.	-60.	36.82	5341.	-1.36	-198.	0.

THETA = 0. PHI = 40.					SIGMA 1		SIGMA 2		ALPHA
EPSILON A	EPSILON B	EPSILON C	EPSILON 1	EPSILON 2	MN/M*M LB/IN*IN		MN/M*M LB/IN*IN		DEG
MICRO M/M	MICRO M/M	MICRO M/M	MICRO M/M	MICRO M/M					
1256.	374.	-508.	1256.	-508.	250.85	36382.	-29.82	-4325.	0.
410.	-66.	-440.	413.	-443.	63.67	9235.	-72.54	-10521.	-3.
370.	-72.	-372.	377.	-379.	59.81	8674.	-60.40	-8760.	-5.
280.	-24.	-236.	284.	-240.	48.20	6991.	-35.20	-5105.	-5.
216.	42.	-130.	216.	-130.	40.23	5835.	-14.82	-2150.	-0.
196.	-84.	-114.	240.	-158.	43.80	6352.	-19.57	-2838.	-19.
174.	56.	-62.	174.	-62.	35.32	5123.	-2.23	-323.	0.

DATA, PRINCIPAL STRAINS, STRESSES, AND ANGLE  
FOR A 44500 N (10000 LB) LOAD ON 127 MM (5 IN) OD  
DOUBLE WEBBED 50 PERCENT MASS REDUCTION MODEL INTERIOR

TABLE 2f

THETA = 90. PHI = 0.					SIGMA 1		SIGMA 2		ALPHA
EPSILON A	EPSILON B	EPSILON C	EPSILON 1	EPSILON 2	MN/M*M	LB/IN*IN	MN/M*M	LB/IN*IN	DEG
MICRO M/M	MICRO M/M	MICRO M/M	MICRO M/M	MICRO M/M					
-156.	-50.	56.	56.	-156.	2.09	303.	-31.64	-4589.	0.
-208.	122.	282.	296.	-222.	52.19	7570.	-30.33	-4399.	-10.
-220.	-78.	52.	52.	-220.	-3.16	-458.	-46.48	-6742.	-1.
-214.	-74.	52.	52.	-214.	-2.74	-398.	-45.13	-6545.	-2.
-220.	-78.	52.	52.	-220.	-3.16	-458.	-46.48	-6742.	-1.
-208.	122.	282.	296.	-222.	52.19	7570.	-30.33	-4399.	-10.
-156.	-50.	56.	56.	-156.	2.09	303.	-31.64	-4589.	0.

THETA = 90. PHI = 20.					SIGMA 1		SIGMA 2		ALPHA
EPSILON A	EPSILON B	EPSILON C	EPSILON 1	EPSILON 2	MN/M*M	LB/IN*IN	MN/M*M	LB/IN*IN	DEG
MICRO M/M	MICRO M/M	MICRO M/M	MICRO M/M	MICRO M/M					
-174.	-68.	38.	38.	-174.	-3.23	-468.	-36.96	-5360.	0.
-348.	276.	296.	415.	-467.	62.56	9073.	-77.92	-11302.	-22.
-348.	-104.	42.	48.	-354.	-13.22	-1917.	-77.20	-11197.	-7.
-202.	-114.	40.	44.	-206.	-3.98	-577.	-43.89	-6366.	8.
-348.	-104.	42.	48.	-354.	-13.22	-1917.	-77.20	-11197.	-7.
-348.	276.	296.	415.	-467.	62.56	9073.	-77.92	-11302.	-22.
-174.	-68.	38.	38.	-174.	-3.23	-468.	-36.96	-5360.	0.

THETA = 90. PHI = 40.					SIGMA 1		SIGMA 2		ALPHA
EPSILON A	EPSILON B	EPSILON C	EPSILON 1	EPSILON 2	MN/M*M	LB/IN*IN	MN/M*M	LB/IN*IN	DEG
MICRO M/M	MICRO M/M	MICRO M/M	MICRO M/M	MICRO M/M					
-174.	-69.	36.	36.	-174.	-3.68	-534.	-37.10	-5380.	0.
-178.	412.	300.	486.	-364.	85.59	12414.	-49.54	-7185.	-28.
-166.	-118.	28.	40.	-178.	-3.10	-449.	-37.68	-5465.	13.
-156.	-126.	28.	47.	-175.	-1.26	-183.	-36.56	-5303.	17.
-166.	-118.	28.	40.	-178.	-3.10	-449.	-37.68	-5465.	13.
-178.	412.	300.	486.	-364.	85.59	12414.	-49.54	-7185.	-28.
-174.	-69.	36.	36.	-174.	-3.68	-534.	-37.10	-5380.	0.